Suitably impressive thesis title

Mikkel Bjørn
St. Anne's College
University of Oxford

A thesis submitted for the degree of
Doctor of Philosophy
Trinity 2020

Acknowledgements

I would very much like to thank myself, for doing such a huge and impressive amount of work.

Abstract

Oh my have I done a lot of things. I have made the best measurement of γ evah! I'll describe that in more detail at an appropriate time.

Contents

Preface

The work presented in this thesis has been resulted in two papers, either under review or published in the Journal of High Energy Physics. These are

> [1] *Measurement of the CKM angle γ using $B^\pm \to [K^0_S h^+ h^-]_D h^\pm$ decays*, submitted to JHEP.
> This paper describes a measurement of the CKM angle γ using pp collision data taken with the LHCb experiment during the Run 1 of the LHC, in 2011 and 2012, and during the full Run 2, in 2015–2018. The measurement uses the decay channels $B^\pm \to Dh^\pm$ where $D \to K^0_S h'^+ h'^-$, in which h and h' denotes pions or kaons. It obtains a value of $\gamma = (?\pm?)^\circ$, which constitutes the world's best single-measurement determination of γ. The work is the main focus of this thesis and described in detail in Chapter 5.

> [2] *CP violation and material interaction of neutral kaons in measurements of the CKM angle γ using $B^\pm \to DK^\pm$ decays where $D \to K^0_S \pi^+ \pi^-$*, JHEP 19 (2020) 106.
> This paper describes a phenomenological study of the impact of neutral kaon *CP* violation and material interaction on measurements of γ. With the increased measurement precision to come in the near future, an understanding of these effects is crucial, especially in the context of $B \to D\pi$ decays; however no detailed study had been published at the start of this thesis. The study is the subject of Chapter 4.

All of the work described in this thesis is my own, except where clearly referenced to others. Furthermore, I contributed significantly to an analysis of $B^\pm \to DK^\pm$ decays with LHCb data taken in 2015 and 2016, now published in

> [3] *Measurement of the CKM angle γ using $B^\pm \to DK^\pm$ with $D \to K^0_S \pi^+ \pi^-$ $K^0_S K^+ K^-$ decays*, JHEP 08 (2018) 176.

I was responsible for the analysis of the signal channel, whereas the control channel was analysed by Nathan Jurik. The measurement is superseded by that of Ref. [1] and is not described in detail in the thesis.

Le roi est mort, vive le roi!

— Traditional French proclamation at the death of one monarch and the ascension of a new

1 Introduction

"The King is dead, long live the King!". Idea of the quote: the Standard Model is dead but, unlike French monarchs, sadly lives on forever. What a conundrum.

Some savoury flavour text on why precision flavour physics is important, and where it fits into the grand scheme of things. Can this be made sexy? Good question.

1.1 Structure of the thesis

2

Theoretical background

This chapter lays out the theoretical framework of the thesis. Section 2.1 introduces charge and parity symmetry violation in general, while Section 2.2 covers the description in the Standard Model and the general theory behind charge-parity symmetry violation measurements in charged B decays. Section 2.3 focuses on the theory of measurements using $B^{\pm} \to Dh^{\pm}$ decays with multi-body D final states, after which the specific analysis strategy for the measurement described in the thesis is laid out in Section 2.4.

2.1 The C, P and T symmetries and their violation

The concept of symmetry play a fundamental role in modern physics. By Noether's theorem [], the simple assumption of invariance of our physical laws under universal temporal and spatial translations leads to the very non-trivial prediction of conserved energy and momentum; within the field of particle physics, the interactions and dynamics of the Standard Model (SM) follow completely simply from requiring the fundamental particle fields to satisfy a local $U(1) \times SU(2) \times SU(3)$ gauge symmetry []; and one of the short-comings of the SM,is that it fails to explain the apparent lack of symmetry in our matter-dominated universe.Indeed, it is important to experimentally establish the symmetries of our world at a fundamental level, and the degree to which they are broken.

I'll adjust this paragraph when I've written the introduction.

Three discrete symmetries of importance are the symmetries under

1. The charge operator C, which conjugates all internal quantum numbers of a quantum state and thus converts particles into their anti-particle counter parts. For example, C transforms the electric charge of a particle state $Q \to -Q$.

2. The parity operator P, which inverts the spatial dimensions of space time: $\vec{x} \to -\vec{x}$. As such, it transforms left-handed particle fields into right-handed particle fields and vice versa.

3. The time-inversion operator T, which inverts the temporal dimension of space time: $t \to -t$.

These are fundamentally related by the CPT theorem [] , which states that any Lorentz-invariant Quantum Field Theory (QFT) must be symmetric under the simultaneous application of *all* three operators. However, any one of the symmetries can be broken individually, and experiments have shown the physical laws of our world to violate each of the C, P, and T symmetries.

This was first established in 1956, when Chien-Shiung Wu observed parity violation in weak decays of Co-60 nuclei [], by carrying out an experiment that was proposed by Yang Chen-Ning and Tsung-Dao Lee []. While this experiment established the breaking of P symmetry, it left open the possibility that the physical world would be left invariant under a combination of a charge- and parity inversion; that it was CP symmetric. However, this was disproved in 1964 when Kronin and Fitch observed that long-lived kaons, which predominantly decay to the CP-odd 3π state, could also decay to the CP-even $\pi\pi$ states [].

Since then CP violation has been found in the B^0 and $B^\pm$ system by the BaBar and Belle collaborations during the early 2000's [], and in the B_s^0 system by LHCb in 2013 []; within the last year and a half the first observation of CP-violation in D^0 decays has been made by the LHCb collaboration [], and most recently evidence for CP-violation in the neutrino sector has been reported by the T2K collaboration []. The observed effects can be divided into distinct classes. The conceptually simplest case is

1. *CP-violation in decay*, where $|A/\bar{A}| \neq 1$ for a decay amplitude A, and the amplitude $\bar{A}$ of the CP-conjugate decay. The result is different decay rates in two CP-conjugate decays

$$\Gamma(M \to f) \neq \Gamma(\bar{M} \to \bar{f}). \tag{2.1}$$

   This type of CP violation was not established until 1988 [], 24 years after the first observation of CP violation, and also this discovery was in $K \to \pi\pi$ decays.

CP-violation in decay is the only type possible for charged initial states, and it is thus the main focus of the thesis. Two additional *CP*-violating effect are possible for neutral initial states (a situation that will be the main focus of Chapter 4). These effects are

2. *CP-violation in mixing*, which denotes the case where the mixing rates between the M^0 and $\bar{M}^0$ states differ

$$\Gamma(M^0 \to \bar{M}^0) \neq \Gamma(\bar{M}^0 \to M^0). \tag{2.2}$$

   The *CP* violation first observed by Kronin and Fitch in the neutral kaon sector [] is (dominantly) of this type.

3. *CP-violation in interference between mixing and decay*, which can be present for a neutral initial states M^0 decaying into a final state f common to both M^0 and $\bar{M}^0$. The decay rate includes an interference term between two amplitudes: the amplitude for a direct $M^0 \to f$ decay and the amplitude for a decay after mixing: $M^0 \to \bar{M}^0 \to f$. Even in the absence of the two aforementioned effects, the rates $\Gamma(M^0 \to f)$ and $\Gamma(\bar{M}^0 \to \bar{f})$ can differ due to the interference term. Such *CP* asymmetries have been measured in eg. $B^0 \to J/\psi K$ [] and $B_s^0 \to J/\psi\phi$ decays [].

CP violation measurements thus have a long, rich, and still-developing history.

2.2 CP violation in the Standard Model

All existing measurements of *CP* violation in the quark sector are naturally explained in the SM; indeed, the need to explain the observation *CP* violation in neutral kaons was a driving force in the development of the model in the first place, when it lead Kobayashi and Maskawa to predict the existence of then-unknown particles in 1973 [] (now known to be the third generation quarks). This section briefly explains the mechanism behind *CP* violation in the SM and then details the current state-of affairs in precision measurements of the fundamental parameter governing the effect: the *CP*-violating phase γ.

2.2.1 The CKM matrix and the Unitarity Triangle

The SM contains three generations of quarks, each consisting of an up-type quark (u, c, and t) and a down-type quark (d, s, and b). The charged weak interaction of the $W^{\pm}$ boson couples up and down-type quarks. The quark states that couple to the W are not (a priori) identical to the mass eigenstates, and can be denoted (u', c', and t') and (d', s', and b'). A basis for the quark states can be chosen such that the weakly coupling up-quark states are identical to the propagating quark states, $u = u'$, but then the down-type quark stare are different: $d' \neq d$. The two bases of the down-type quarks are related via the CKM matrix[1]

$$\begin{pmatrix} d' \\ s' \\ t' \end{pmatrix} = V \begin{pmatrix} d \\ s \\ t \end{pmatrix} = \begin{pmatrix} V_{ud} & V_{us} & V_{ub} \\ V_{cd} & V_{cs} & V_{cb} \\ V_{td} & V_{ts} & V_{tb} \end{pmatrix} \begin{pmatrix} d \\ s \\ t \end{pmatrix}. \tag{2.3}$$

Thus the Lagrangian terms representing the coupling of a $W^{\pm}$ boson with a u- and a d-type quark is

$$\mathcal{L}_{W^+} = -\frac{g}{\sqrt{2}} V_{ud} \left(\bar{u} \gamma^{\mu} W_{\mu}^{+} d \right) \qquad \mathcal{L}_{W^-} = -\frac{g}{\sqrt{2}} V_{ud}^{*} \left(\bar{d} \gamma^{\mu} W_{\mu}^{-} u \right) \tag{2.4}$$

where g is the weak coupling constant, γ_u are the Dirac matrices, and u and d represent the left-handed components of the physical quark states.

The CKM matrix is a unitary complex 3×3 matrix, and hence has $3^2 = 9$ independent, real parameters. However, 5 of these can be absorbed into unphysical phases of the quark states (both mass and weak eigenstates) and hence the matrix has 4 real, physical parameters: 3 mixing angles and a single phase [**?**]. Chau and Keung [] proposed the parameterisation

$$\begin{aligned} V &= \begin{pmatrix} 1 & 0 & 0 \\ 0 & c_{23} & s_{23} \\ 0 & -s_{23} & c_{23} \end{pmatrix} \begin{pmatrix} c_{13} & 0 & s_{13} e^{-i\delta_{CP}} \\ 0 & 1 & 0 \\ -s_{13} e^{-i\delta_{CP}} & 0 & c_{13} \end{pmatrix} \begin{pmatrix} c_{12} & s_{12} & 0 \\ -s_{12} & c_{12} & 1 \\ 0 & 0 & 1 \end{pmatrix} \\ &= \begin{pmatrix} c_{12}c_{13} & s_{12}c_{13} & s_{13} e^{-i\delta_{CP}} \\ -s_{12}c_{23} - c_{12}s_{23}s_{13} e^{i\delta_{CP}} & c_{12}c_{23} - s_{12}s_{23}s_{13} e^{i\delta_{CP}} & s_{23}c_{13} \\ s_{12}s_{23} - c_{12}c_{23}s_{13} e^{i\delta_{CP}} & -c_{12}s_{23} - s_{12}c_{23}s_{13} e^{i\delta_{CP}} & c_{23}c_{13} \end{pmatrix} \end{aligned} \tag{2.5}$$

which is the preferred standard by the PDG []. Here, $s_{ij} \equiv \sin\theta_{ij}$ and $c_{ij} \equiv \cos\theta_{ij}$ denote the sine and cosine of three rotation angles in quark space; $\theta_{ij} = \theta_C = X$ [] being the usual Cabibbo angle [].

[1] A basis for the quarks can of course be chosen, such that neither the up-quarks or the down-quarks are expressed in their mass eigenstates. In that case the CKM matrix is recovered as $V = U_u^* U_d$, where $U_{u/d}$ is the unitary transformation matrices that brings the u/d quarks into their mass eigenstates.

The presence of the complex phase δ_{CP} in the Lagrangian term of the W coupling causes *CP* violation because, as evident from Eq. **??**, if δ_{CP} enters the amplitude for some decay mediated by a W boson, $A = |A|e^{i(\delta_0+\delta_{CP})}$, then it will enter the *CP* conjugate decay amplitude with the opposite sign: $\bar{A} = |A|e^{i(\delta_0-\delta_{CP})}$. In these expressions, δ_0 denotes a *CP* conserving phase that is not caused by complex terms in the Lagrangian, but arises due to potential intermediate states in the decay amplitude.[2] Usually the underlying mechanism is due to QCD effects, and these *CP* conserving phases are therefore generally dubbed *strong* phases, as opposed to the *CP* violating *weak* phase of the W coupling [**?**]. This terminology will be applied throughout the thesis.

Experimentally, it has been observed that the CKM matrix elements of Eq. (2.5) satisfy $s_{13} \ll s_{23} \ll s_{12}$. This motivates an often used, alternative parameterisation of the matrix, where the elements are expressed as power series in a parameter λ that naturally incorporates this hierarchy: the Wolfenstein parameterisation []. The definitions

$$\begin{aligned} s_{12} &\equiv \lambda \\ s_{23} &\equiv \lambda^2 A \\ s_{13} &\equiv \lambda^3(\rho - i\eta) \end{aligned} \tag{2.6}$$

are made, after which the unitarity conditions (or Eq. 2.5) determine the remaining elements to any order in λ.[3] To $\mathcal{O}(\lambda^5)$ the Wolfenstein parameterisation of the CKM matrix is [**?**, 5]

$$V = \begin{pmatrix} 1 - \frac{\lambda^2}{2} - \frac{\lambda^4}{8} & \lambda & A\lambda^3(\rho - i\eta) \\ -\lambda + \frac{\lambda^5}{2}A^2(1 - 2(\rho + i\eta)) & 1 - \frac{\lambda^2}{2} - \frac{\lambda^4}{8}(1 + 4A^2) & A\lambda^2 \\ A\lambda^3(1 - (\rho + i\eta)(1 - \frac{\lambda^2}{2})) & -A\lambda^2(1 - \frac{\lambda^2}{2}(1 - 2(\rho + i\eta))) & 1 - \frac{1}{2}A^2\lambda^4 \end{pmatrix}. \tag{2.7}$$

The unitarity condition $V^\dagger V = \mathbb{1}$ of the CKM matrix defines 9 relations between the CKM elements of the form

$$\sum_j V_{jq}^* V_{jq} = 1 \quad , \quad q \in \{d, s, b\} \qquad \text{along the diagonal} \tag{2.8a}$$

$$\sum_j V_{jq}^* V_{jq'} = 0 \quad , \quad q, q' \in \{d, s, b\}, q \neq q' \qquad \text{off-diagonal.} \tag{2.8b}$$

[2] It is generally true that all phases of a single term in a given amplitude will be convention dependent, but that the phase differences between terms are not.

[3] Other variants of the Wolfenstein parameterisation do exist [4]. They all agree at the lowest orders of λ.

Figure 2.1: Caption here

The off-diagonal conditions constrain three complex numbers to sum to zero, and can thus be visualised as triangles in the complex plane, the so-called unitarity triangles. Of these, the triangle corresponding to the (d, b) elements plays a special role, because all three sides are of the same order of magnitude, $\mathcal{O}(\lambda^3)$. When expressed in the form

$$\frac{V_{ud}^* V_{ub}}{V_{cd}^* V_{cb}} + \frac{V_{td}^* V_{tb}}{V_{cd}^* V_{cb}} + 1 = 0, \tag{2.9}$$

it is often referred to as the singular Unitarity Triangle, illustrated in Fig. 2.1 where the usual names for the three angles are also given.

Over-constraining the unitarity triangle by making separate measurements of all sides and angles, in as many different decay channels as possible, is an important, and non-trivial test of the SM. The current experimental constraints are in agreement with the SM predictions, as visualised in Fig. 2.2. The CKM angle

$$\gamma \equiv \arg(-V_{ud}V_{ub}^*/V_{cd}V_{cb}^*) = \arg(-V_{cb}V_{cd}^*/V_{ub}V_{ud}^*) \tag{2.10}$$

is unique among the CKM parameters, in that it can be measured in tree-level processes without significant theoretical uncertainty from lattice QCD calculations []. Because tree-level processes are less likely to be affected by Beyond-Standard-Model (BSM) effects, direct measurements of γ can be considered a SM benchmark, which can be compared to estimates based on measurements of other CKM elements that are measured in loop-level processes, and thus are more likely to be affected by BSM effects [**?**]. The current, worldwide combination of direct measurements, published by the CKMFitter group, is $\gamma = (72.1^{+5.4}_{-5.7})^\circ$, to be compared with the estimate from loop-level observables of $\gamma = (65.6^{+1.0}_{-3.4})^\circ$ [**?**]. Other world averages exist [**?**, **?**], but the overall picture is the same: the ability to constrain BSM physics is currently limited by the uncertainty of the direct measurements. Hence further precision measurements of γ are highly motivated. Presently, the precision is driven by time-integrated measurements if direct *CP*-violation in $B^\pm \to DK^\pm$ decays; such a measurement is the topic of this thesis and the topic is treated in detail in the following section. It is also possible to measure γ in time-dependent mixing analyses of X, Y, and related decays, by measuring *CP* violation in interference between mixing and decay. These modes are expected to provide competitive measurements in the future [].

Not sure if I should spend time explaining the non-gamma measurements entering?

make sure these are up to data (probably not the case)

Figure 2.2: Caption here

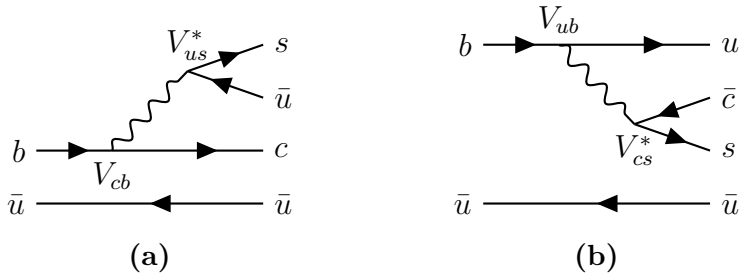

Figure 2.3: Tree level Feynman diagrams describing (a) $B^- \to D^0 K^-$ and (b) $B^- \to \overline{D}^0 K^-$ decays. The electro-weak phase difference between the two decays is $\Delta\phi = \arg\left(V_{cb}V_{us}^*/V_{ub}V_{cs}^*\right) \simeq \gamma$.

2.2.2 Measuring γ in tree level decays

The phase γ can be measured in tree-level processes with interference between $b \to cs\bar{u}$ and $b \to \bar{c}su$ transitions. The canonical example, also the subject of this thesis, is based on measurements sensitive to interference between the $B^\pm \to D^0 K^\pm$ and $B^\pm \to \overline{D}^0 K^\pm$ decay amplitudes. As illustrated in Fig. 2.3 for the case of B^- decays, the electro-weak phase difference between the two decays is $\Delta\phi = \arg\left(V_{cb}V_{us}^*/V_{ub}V_{cs}^*\right)$. While $\Delta\phi$ is not identical to the definition of γ in Eq. (2.10), the ratio of the involved CKM matrix elements is [6]

$$\begin{aligned} -\frac{V_{cd}^*/V_{ud}^*}{V_{us}^*/V_{cs}^*} &= -\frac{-\lambda[1-\frac{\lambda^4}{2}A^2(1-2(\rho-i\eta))](1-\frac{\lambda^2}{2}-\frac{\lambda^4}{8}(1+4A^2))}{\lambda(1-\frac{\lambda^2}{2}-\frac{\lambda^4}{4})} \\ &= 1-\lambda^4A^2(1-2(\rho-i\eta))+\mathcal{O}(\lambda^5). \end{aligned} \tag{2.11}$$

The ratio equals unity to $\mathcal{O}(\lambda^4) \simeq 2.6 \times 10^{-3}$, and thus $\Delta\phi \simeq \gamma$ is a good approximation within current experimental uncertainties. For the remainder of this thesis the approximation will be used without further comment. The diagrams in Fig. 2.3 describe the leading order contributions to the two amplitudes

$$\begin{aligned} A[B^- \to D^0 K^-] &\equiv A_B \\ A[B^- \to \overline{D}^0 K^-] &\equiv \bar{A}_B \equiv r_B A_B e^{i(\delta_B-\gamma)}, \end{aligned} \tag{2.12a}$$

where the last equality introduces two new parameters: the amplitude magnitude ratio $r_B \equiv |\bar{A}_B|/|A_B|$, and δ_B, the strong-phase difference between the decay amplitudes. Since all *CP*-violation is attributed to the electro-weak phase in the SM, the *CP*-conjugate decay amplitudes are [7]

$$\begin{aligned} A[B^+ \to \overline{D}^0 K^+] &= A_B \\ A[B^+ \to D^0 K^+] &= \bar{A}_B = r_B A_B e^{i(\delta_B+\gamma)}. \end{aligned} \tag{2.12b}$$

In an experimental setting, the D^0 and $\overline{D}^0$ mesons are reconstructed in some final state, f or its *CP*-conjugate $\bar{f}$. In analogy with the $B^\pm$ decays, the D decay amplitude can be related[4]

$$\begin{aligned} A[D^0 \to f] &= A[\overline{D}^0 \to \bar{f}] = A_D \\ A[\overline{D}^0 \to f] &= A[D^0 \to \bar{f}] = r_D A_D e^{i\delta_D}. \end{aligned} \tag{2.13}$$

where the assumption has been made that there is no *CP* violation in the D decays, and δ_D denotes a *CP*-conserving strong-phase difference. While *CP*-violation in D decays has recently been measured [], the size of the effect is small and it is considered negligible in this thesis. Based on Eqs. 2.12 and (2.13), the decay rates of B^+ and B^- mesons into the possible final states can be seen to satisfy

$$\Gamma(B^- \to D(\to f)K^-) \propto 1 + r_D^2 r_B^2 + 2r_B r_D \cos\left[\delta_B + \delta_D - \gamma\right], \tag{2.14a}$$

$$\Gamma(B^+ \to D(\to \bar{f})K^+) \propto 1 + r_D^2 r_B^2 + 2r_B r_D \cos\left[\delta_B + \delta_D + \gamma\right], \tag{2.14b}$$

$$\Gamma(B^- \to D(\to \bar{f})K^-) \propto r_D^2 + \ r_B^2 + 2r_B r_D \cos\left[\delta_B - \delta_D - \gamma\right], \tag{2.14c}$$

$$\Gamma(B^+ \to D(\to f)K^+) \propto r_D^2 + \ r_B^2 + 2r_B r_D \cos\left[\delta_B - \delta_D + \gamma\right]. \tag{2.14d}$$

The processes in Eqs. (2.14a) and (2.14b) are *CP*-conjugate and it is clear how, in the typical case where $\delta_B + \delta_D \neq 0$, a non-zero value of γ leads to *CP* violation in the form of differing decay rates. The same is true for the processes in Eqs. (2.14c) and (2.14d). Depending on the choice of D final state, these expressions can be used to relate γ to various observables that are experimentally accessible. This thesis concerns the choice $f = K^0_S\pi^+\pi^-$ or $f = K^0_S K^+ K^-$, where the terms related to the D decay all have a non-trivial variation over the phase space of the decay. However, it is useful to first analyse the simpler case where f is a two-body state.

The simplest case is when f is chosen to be a *CP* eigenstate, so that $f = \pm\bar{f}$ and the rate equations of (2.14a)–(2.14d) simplify, because $r_D = 1$ and $\delta_D \in \{0, \pi\}$. Measurements of γ in such decay modes are denoted GLW measurements, after Gronau, London, and Wyler who described the approach in the early 90ies [7, 8]. Experimentally it is preferable to measure yield ratios rather than absolute rates, and the observables of interest are thus the *CP* asymmetry

$$\begin{aligned} A_{CP=\pm1} &= \frac{\Gamma[B^- \to D_{CP}K^-] - \Gamma[B^+ \to D_{CP}K^+]}{\Gamma[B^- \to D_{CP}K^-] + \Gamma[B^+ \to D_{CP}K^+]} \\ &= \frac{\pm r_B \sin\delta_B \sin\gamma}{1 + r_B^2 \pm 2r_B \cos\delta_B \cos\gamma}, \end{aligned} \tag{2.15a}$$

[4] In this notation δ_D is thus phase of the suppressed D-decay amplitude minus the phase of the favoured D-decay amplitude. This is the opposite convention to that used in the LHCb measurements with the ADS technique [], but aligns with the notation used in the literature on γ measurements in $D \to K^0_S\pi^+\pi^-$ decays [].

Figure 2.4: Caption here

as well as the ratio

$$\begin{aligned} R_{CP=\pm1} &= 2\frac{\Gamma[B^- \to D_{CP}K^-] + \Gamma[B^+ \to D_{CP}K^+]}{\Gamma[B^- \to D^0K^-] + \Gamma[B^+ \to \overline{D}^0K^+]} \\ &= 1 + r_B^2 \pm 2r_B \cos\delta_B \cos\gamma. \end{aligned} \tag{2.15b}$$

In practice, A_{CP} and R_{CP} are obtained from measured yield ratios that are corrected with appropriate branching fractions. A measurement of A_{CP} and R_{CP} alone is not sufficient to determine the underlying physics parameters (γ, r_B, δ_B), and this is not solely due to the number of parameters exceeding the number of constraints: the equations also allow for multiple, ambiguous solutions for (γ, δ_B). One way to break the ambiguity, first noted in the original paper [7], is to make further measurements in additional B decays. These can be described with the formalism described above, but will not share the same ambiguous solutions because (r_B, δ_B) are unique to a given B decay. Another method is to analyse D decay final states that are not *CP* eigenstates.

In the XX analysed an alternative choice of D final states: a simultaneous analysis of a Cabibbo-favoured (CF) decay $D^0 \to f$ and the doubly-Cabibbo-suppressed (DCS) decay $D^0 \to \bar{f}$ into the *CP* conjugate final state. The classical example is to take $f = K^-\pi^+$ and $\bar{f} = \pi^-K^+$. The relative suppression means that the r_D of Eq. (2.14) is small, typically of the same order of magnitude as r_B, and thus the *CP* asymmetry of the suppressed decay is $\mathcal{O}(1)$:

$$\begin{aligned} A_{ADS(\bar{f})} &= \frac{\Gamma[B^- \to D(\to \bar{f})K^-] - \Gamma[B^+ \to D(\to f)K^+]}{\Gamma[B^- \to D(\to \bar{f})K^-] + \Gamma[B^+ \to D(\to f)K^+]} \\ &= \frac{r_D r_B \sin(\delta_B - \delta_D)\sin\gamma}{r_D^2 + r_B^2 + 2r_D r_B \cos(\delta_B - \delta_D)\cos\gamma}. \end{aligned} \tag{2.16a}$$

The large *CP* asymmetry is a prime feature of the ADS method. However, also the suppressed-to-favoured yield ratio is sensitive to the physics parameters of interest:

$$\begin{aligned} R_{ADS(\bar{f})} &= \frac{\Gamma[B^- \to D(\to \bar{f})K^-] + \Gamma[B^+ \to D(\to f)K^+]}{\Gamma[B^- \to D(\to f)K^-] + \Gamma[B^+ \to D(\to \bar{f})K^+]} \\ &= \frac{r_B^2 + r_D^2 + 2r_D r_B \cos(\delta_B - \delta_D)\cos\gamma}{1 + r_D^2 r_B^2 + 2r_D r_B \cos(\delta_B + \delta_D)\cos\gamma}. \end{aligned} \tag{2.16b}$$

The interpretation of A_{ADS} and R_{ADS} in terms of (γ, r_B, δ_B) requires knowledge of the r_D and δ_D parameters, but these can be measured independently []. In general, the constraints from a single set of ADS observables suffer the same ambiguities as

in the GLW case. However, unlike the GLW case, each D decay mode provides an independent set of constraints, because the parameters related to the D decay vary.

The discussion of this section has centred on the classical case of $B^{\pm} \to DK^{\pm}$ decays with a two-body D final state. With minor modifications the techniques have been used to make measurements of γ in B^0 decays [], with B decay final states including excited D mesons [], excited kaons [], or pions []. The decay $B^{\pm} \to D\pi^{\pm}$ also is also *CP*-violating, although the effect is much smaller than in the $B^{\pm} \to DK^{\pm}$ decay, because $r_B^{D\pi^{\pm}} \simeq 0.005 \sim \mathcal{O}(\lambda^X)$, whereas $r_B^{DK^{\pm}} \simeq 0.1 \sim \mathcal{O}(\lambda^X)$. Furthermore, it is possible to use multi-body D final states []. However, in some cases, a better precision can then be obtained by exploiting phase-space dependent decay rates. This is the topic of the next section.

2.3 Measuring γ using multi-body D final states

In multi-body D decays, the r_D and δ_D parameters of the fundamental rate equations in Eq. (2.14) vary over the phase space of the D decay. This section describes a model-independent approach to measure γ in $B \to D(\to K^0_S\pi^+\pi^-)h^{\pm}$ decays by exploiting this variation. The theory is identical for $D \to K^0_S K^+ K^-$ decays, and similar ideas have been proposed for the $D \to K^0_S\pi^+\pi^-\pi^0$ [] and $D \to 2\pi^+2\pi^-$ modes []. First, however, the formalism for describing amplitudes of multi-body decays is briefly reviewed.

2.3.1 Dalitz plots and the phase space of multibody decays

In general, the phase space of the n-body decay $P \to p_1 + p_2 + ... + p_n$ consists of n four momenta, with a total of $4n$ components. The requirement that each of the final state particles is on-shell provides n constraints on these components, and energy-momentum conservation removes a further 4 degrees of freedom. If the original particle P is s *scalar*, the decay is isotropic, which removes an additional 3 degrees of freedom, leaving the total number of degrees of freedom at $3n-7$. For the specific case of three-body decays, the available phase space can thus be parameterised with only two parameters. A practical and often used choice is the invariant masses

$$s_{12} = m^2(p_1p_2) = (p_1^{\mu} + p_2^{\mu})^2, \qquad s_{13} = m^2(p_1p_3) = (p_1^{\mu} + p_3^{\mu})^2. \tag{2.17}$$

The choice of particle pairs is arbitrary, and the coordinates easily related

$$m_P^2 + m_{p_1}^2 + m_{p_2}^2 + m_{p_3}^2 = m^2(p_1p_2) + m^2(p_1p_3) + m^2(p_2p_3). \tag{2.18}$$

A scatter plot of (s_{12}, s_{13}) values for a sample of particle decays is denoted a Dalitz plot []. It has the very useful feature that the presence of (narrow) resonances in the decay leads to visible bands in the scatter plot. Figure **??** shows an example of a Dalitz plot for $D \to K^0_S\pi^+\pi^-$ decays in which the $K^*(892)^\pm$ and $\rho(770)$ resonances are clearly visible. The plot shows the sample of $B^- \to D\pi^-$ decays used to make the measurement described in Chapter 5 and thus the D meson is in a superposition of D^0 and $\overline{D}^0$ states (as detailed in the following section).

In terms of the coordinates of Eq. (**??**) the differential decay rate is given by [**?**]

$$\mathrm{d}\Gamma = \frac{1}{32(2\pi)^3 m_P^3}|\mathcal{M}|^2\,\mathrm{d}s_{12}\mathrm{d}s_{13}, \tag{2.19}$$

where $\mathcal{M}$ is the QFT matrix element, or total decay amplitude, corresponding to the decay. In general, it is not possible to calculate $\mathcal{M}$ from first principles. Instead, a model is defined with an empirically well motivated form, in which a number of free parameters must be determined experimentally. The simplest case is that of an *isobar* model, where it is assumed that the full decay can be decomposed into consecutive two-body decays of the form $P \to R_{12}(\to p_1 + p_2)p_3$. Thus, $\mathcal{M}$ is expressed as a non-resonant constant amplitude term, k_{NR}, plus a sum of resonance terms

$$\mathcal{M}(s_{12}, s_{13}) = k_{NR} + \sum_r k_r \mathcal{M}^r(s_{12}, s_{13}). \tag{2.20}$$

The exact form of the $\mathcal{M}^r$ function depends on the resonance in question. A detailed review can be found in eg. Ref. []. The isobar formalism breaks down when resonances in the decay are not well separated. In this case, models of the form in Eq. (**??**) can still be employed, if the contribution from overlapping resonances are collected in a single term. An example of such a model, is the amplitude model for $D^0 \to K^0_S\pi^+\pi^-$ decays developed by the Belle collaboration for a measurement of the CKM angle β in 2018 []. In this model, individual terms are included for $D^0 \to K^*(\to K^0_S\pi^\pm)\pi^\mp$ decays, whereas the resonant behaviour of the $\pi\pi$ decay products is modelled with the so-called K-matrix formalism []. The amplitude and phase of $\mathcal{M}$ as predicted by this model are shown in Fig. **??**.

2.3.2 The GGSZ method to measure γ

The non-trivial phase-space dependence of the $D \to K^0_S\pi^+\pi^-$ decay amplitude can be exploited to measure γ with $B^\pm \to DK^\pm$ or $B^\pm \to D\pi^\pm$ decays. For this specific decay, s_- and s_+ are used to described the Dalitz coordinates $m^2(K^0_S\pi^-)$ and $m^2(K^0_S\pi^+)$, respectively, and the D decay amplitude is a function of these coordinates

$$A_S^{(\overline{D})}(s_-, s_+) = A(\overline{D}^{(0)} \to K^0_S\pi^+\pi^-). \tag{2.21}$$

To a good approximation the K^0_S meson is a *CP* eigenstate, meaning that the $K^0_S\pi^+\pi^-$ state is self-conjugate. Assuming this approximation to be exact, and that *CP* violation in the D decay is negligible, the D decay amplitude satisfies the symmetry relation

$$A^{\bar{D}}_S(s_-, s_+) = A^D_S(s_+, s_-). \tag{2.22}$$

The impact of the K^0_S meson *not* being an exact *CP* eigenstate is treated in detail in Chapter 4. In order to simplify equations, the short-hand notation

$$(s_{-+}) = (s_-, s_+), \qquad (s_{+-}) = (s_+, s_-) \tag{2.23}$$

will be employed for the remainder of this thesis, so that the relation in Eq. (2.22) can be expressed as $A^{\bar{D}}_S(s_{-+}) = A^D_S(s_{+-})$. Thus, the rate equations of Eq. (2.14) for the $D \to K^0_S\pi^+\pi^-$ decay mode are

$$\begin{aligned} \mathrm{d}\Gamma^-(\mathrm{s}_{-+}) \propto |\mathcal{A}^-_S|^2 &= |A_B|^2|A_{K^0_S}|^2 \\ &\times \Big[|A^D_S(s_{-+})|^2 + r_B^2|A^D_S(s_{+-})|^2 + 2r_B|A^D_S(s_{-+})||A^D_S(s_{+-})| \\ &\times (\cos[\delta_D(s_{-+})]\cos[\delta_B - \gamma] + \sin[\delta_D(s_{-+})]\sin[\delta_B - \gamma])\Big], \end{aligned} \tag{2.24a}$$

$$\begin{aligned} \mathrm{d}\Gamma^+(\mathrm{s}_{-+}) \propto |\mathcal{A}^+_S|^2 &= |A_B|^2|A_{K^0_S}|^2 \\ &\times \Big[|A^D_S(s_{+-})|^2 + r_B^2|A^D_S(s_{-+})|^2 + 2r_B|A^D_S(s_{-+})||A^D_S(s_{+-})| \\ &\times (\cos[\delta_D(s_{-+})]\cos[\delta_B + \gamma] - \sin[\delta_D(s_{-+})]\sin[\delta_B + \gamma])\Big]. \end{aligned} \tag{2.24b}$$

Here, $\delta_D(s_{-+}) = \phi_D(s_{-+}) - \phi_D(s_{+-}) = -\delta_D(s_{+-})$, where $\phi_D(s_{-+})$ denotes the complex phase of the $A^D_S(s_{-+})$ amplitude, and a standard trigonometric relation have been employed to factorise the terms depending on the complex phases of the B and D decays. It can be seen that in the case where $\gamma = 0$ the B^+ and B^- decay rates are symmetric if the Dalitz coordinates are exchanged: $\Gamma^+(s_-, s_+) = \Gamma^-(s_+, s_-)$. The presence of *CP* violation in the B decay breaks the symmetry. Therefore it is possible to measure γ (and the nuisance parameters r_B and δ_B) from the phase-space distribution of $B^\pm \to D(\to K^0_S\pi^+\pi^-)K^\pm$ decays, given knowledge of $A^D_S(s_{-+})$. A series of measurements of γ have been made that use amplitude models of the D decay [?, ?, ?, ?, ?, ?, 9, 10]. However, the topic of this thesis is a model-independent measurement

Here is where the discussion of model-dependent vs model-independent should

Figure 2.5: Caption here

2.3.3 A model-independent approach

The phase-space distribution can be analysed in a model-independent way, if the D-decay phase space is split into regions, or bins, an the B decay yield in each bin determined experimentally. The binned approach was featured in the original GGSZ paper [] and the model-independent approach developed further in Refs. []. A measurement of γ using this approach is the main topic of the thesis. This section describes the fundamental principle, whereas the details pertaining to the exact experimental approach are delegated to Section **??**.

The amplitude symmetry of Eq. (2.22) is exploited by defining $2N$ bins to be symmetric symmetric around the $s_- = s_+$ diagonal of the Dalitz plot, numbered $i = -N$ to N (omitting zero) such that if the point (s_-, s_+) is in bin i, then (s_+, s_-) is in bin $-i$, and by convention $i > 0$ for bins where $s_- > s_+$. The principle is illustrated in Fig. 2.5, but the binning schemes used in actual measurements are more complicated. The decay rates in Eq. (**??**) can be integrated over such bins, and give the bin yields

$$\begin{aligned} N_i^- &\propto h^- \left[K_i + r_B^2 K_{-i} + 2\sqrt{K_i K_{-i}} \left(c_i x_- + s_i y_- \right) \right], \\ N_i^+ &\propto h^+ \left[K_{-i} + r_B^2 K_i + 2\sqrt{K_i K_{-i}} \left(c_i x_+ - s_i y_+ \right) \right], \end{aligned} \tag{2.25}$$

where the parameters describing the B decay have been expressed in terms of the observables

$$x_\pm = r_B \cos(\delta_B \pm \gamma), \qquad y_\pm = r_B \sin(\delta_B \pm \gamma), \tag{2.26}$$

and a number of phase-space integrated quantities related to the D-decay have been introduced. The K_i parameters denote fractional yield of a flavour-tagged D^0 decaying into bin i, defined as

$$K_i = \frac{1}{N_K} \int_i \mathrm{d}s^2 |A_\mathrm{S}^D(s_{-+})|^2, \qquad N_K = \int \mathrm{d}s^2 |A_\mathrm{S}^D(s_{-+})|^2, \tag{2.27}$$

where $\int_i \mathrm{d}s^2$ denotes integration over bin i of the Dalitz plot. The c_i and s_i denote the amplitude-weigthed average of $\cos\delta_D(s_{-+})$ and $\sin\delta_D(s_{-+})$ over bin i

$$\begin{aligned} c_i &= \frac{\int_i \mathrm{d}s^2 |A_\mathrm{S}^D(s_{-+})||A_\mathrm{S}^D(s_{+-})| \cos[\delta_D(s_{-+})]}{\sqrt{\int_i \mathrm{d}s^2 |A_\mathrm{S}^D(s_{-+})|^2} \sqrt{\int_i \mathrm{d}s^2 |A_\mathrm{S}^D(s_{+-})|^2}}, \\ s_i &= \frac{\int_i \mathrm{d}s^2 |A_\mathrm{S}^D(s_{-+})||A_\mathrm{S}^D(s_{+-})| \sin[\delta_D(s_{-+})]}{\sqrt{\int_i \mathrm{d}s^2 |A_\mathrm{S}^D(s_{-+})|^2} \sqrt{\int_i \mathrm{d}s^2 |A_\mathrm{S}^D(s_{+-})|^2}}. \end{aligned} \tag{2.28}$$

By the symmetry properties of $\delta_D(s_{-+})$ these parameters satisfy $c_i = c_{-i}$ and $s_i = -s_{-i}$. The normalisation constants h^+ and h^- are identical in the ideal case, but it is convenient to keep define them separately for practical reasons: depending on the experimental setup, there may be overall production and detection asymmetries that affect the total signal yields. An experimental analysis can be made insensitive to these effects because they can be absorbed into the normalisation constants, as long as they are constant over the D-decay phase space. This comes at the cost that the information on $x_\pm$ and $y_\pm$ from the overall CP asymmetry is lost, but Section 2.3.5 will show that the loss in precision is minimal.

Thus, for a set of $2N$ bins, the bin yields of Eqs. (2.25) provide $4N$ constraints on a total of $4N + 6$ parameters: $(h^\pm, K_i, c_i, s_i, x_\pm, y_\pm)$. However, the K_i, c_i, and s_i parameters relate only to the D decay, and can thus, in principle, be measured in independent experiments. With such external inputs a measurement of the $B^\pm \to D(\to K^0_S\pi^+\pi^-)K^\pm$ yields in a set of bins can be used to constrain $x_\pm$ and $y_\pm$, and thereby (γ, r_B, δ_B). The measurement presented in this thesis determines the K_i parameters directly, but uses externally measured values of c_i and s_i as input, as measured in quantum correlated D decays by the CLEO [] and BESIII [] collaborations. Because these measurements are the foundation of the approach, they are described in some detail in the following section.

2.3.4 Measuring strong-phase inputs at charm factories

The strong-phase parameters c_i and s_i have been measured by the CLEO and BESIII collaborations, using quantum correlated $D^0\overline{D}^0$ pairs from decays of the $\psi(3770)$ resonance state, itself produced in e^+e^- collisions at the resonance energy. The $\psi(3770)$ has quantum-number $C = -1$, which is conserved in the strong decay into two D mesons, and thus the two D mesons are produced in an anti-symmetric wave function. By observing the decay of one D meson into a specific final state, say a CP eigenstate, the quantum state of the other D meson can be determined. The measurement is based on decays where both D decays are reconstructed, one in the $K^0_S\pi^+\pi^-$ final state, the other in one of several different tag categories. The main principles are outlined below, but most experimental considerations and implementation details are left out for the sake of brevity.

The simplest case is when one D meson decays into a final state that uniquely tags the flavour, such as $\overline{D}^0 \to K^+e^-\bar{\nu}_e$. In that case, the D meson decaying to $K^0_S\pi^+\pi^-$ is known to be in the D^0 state and the decay rate is simply determined by $A^D_S : \Gamma(s_{-+}) \propto |A^D_S(s_{-+})|^2$. This allows for a measurement of the K_i parameters.

If one D meson is reconstructed in a CP-even state, eg. K^+K^-, or a CP-odd state, eg. $K^0_S\pi^0$, the D meson decaying to $K^0_S\pi^+\pi^-$ is known to be in a state of opposite CP. Thus, for a tag-decay of $CP = \pm 1$ the decay rate has the form

$$\Gamma_{CP=\pm1} \propto \left|A^D_S(s_{-+}) \mp A^D_S(s_{+-})\right|^2 \tag{2.29a}$$

and the bin yields will be given by

$$M^\pm_i \propto K_i + K_{-i} \mp 2\sqrt{K_iK_{-i}}c_i. \tag{2.29b}$$

Thus a simultaneous analysis of flavour and CP tagged decays allow for a determination of the K_i and c_i parameter sets.

Finally, the case where both D mesons, for now denoted D and D', decay into the $K^0_S\pi\pi$ final state can be considered. The total amplitudes have contributions from the case where D is in the D^0 state and D' is in the $\overline{D}^0$ state, as well as the opposite flavour assignment. Thus the decay rate satisfies

$$\Gamma_{CP=\pm1} \propto \left|A^D_S(s_{-+})A^D_S(s'_{+-}) + A^D_S(s_{+-})A^D_S(s'_{-+})\right|^2 \tag{2.30a}$$

where s_{-+} denotes the Dalitz-plot coordinates of the D meson, and s'_{-+} those of the D' meson. Defining M_{ij} to be the yield of decays where the D decay is in bin i and the D' in bin j, the bin yields satisfy

$$M_{ij} \propto K_iK_{-j} + K_jK_{-i} - 2\sqrt{K_iK_{-i}K_jK_{-j}}\,(c_ic_j + s_is_j)\,. \tag{2.30b}$$

Thus, analysing these decays in addition to the CP and flavour tagged decays provide information on all of K_i, c_i, and s_i. Note, however, that Eqs. (2.29a) and (2.30) are invariant under the transformation $\delta_D \to -\delta_D$. In practice, the analysis is extended in a number of ways to enhance the statistics: using "flavour-tag" states that are not exact flavour tags, such as $K^-\pi^+$, using self-conjugate multi-body D-decay final states that are not exact CP eigenstates, such as $\pi^+\pi^-\pi^0$, and using the $K^0_L\pi^+\pi^-$ final state as well. However, the main principles are the same as described above.

Where exactly is this phase sign know from? Is the overall sign not arbitrary in amplitude models?

The measurements of c_i and s_i are made for a range of different binning schemes. It was noted already in Ref. [] that a rectangular binning scheme, such as the example in Fig. **??**, does not provide the optimal sensitivity to γ. A better sensitivity can be obtained if the bins are defined such that δ_D is approximately constant over a given bin, by defining bin i out of N via the condition

$$\text{bin}_i = \{(s_-, s_+) \quad | \quad 2\pi(i-3/2)/N \,<\, \delta_D(s_-, s_+) \,<\, 2\pi \times (i-1/2)/N\}\,. \tag{2.31}$$

In practice, the binning scheme is defined by splitting the D-decay phase-space into quadratic *micro bins* with a width of X (GeV/c^2)^2 and assigning a bin number to each micro bin via the condition in (2.31) as evaluated in an amplitude model of choice. The obtained binning scheme when using an amplitude model developed by the BaBar collaboration in 2008 [] is shown in Fig. **??**. In Ref [] it was also shown that the binning can be even further optimised for sensitivity. The suggested figure of merit is

$$Q^2 = \frac{\sum_i \left(\frac{1}{\sqrt{N_i^B}}\frac{\mathrm{d}N_i^B}{\mathrm{d}x}\right)^2 + \left(\frac{1}{\sqrt{N_i^B}}\frac{\mathrm{d}N_i^B}{\mathrm{d}y}\right)^2}{\int \mathrm{d}s^2 \left[\left(\frac{1}{|\Gamma^B(s_{-+})|}\frac{\mathrm{d}|\Gamma^B(s_{-+})|^2}{\mathrm{d}x}\right)^2 + \left(\frac{1}{|\Gamma^B(s_{-+})|}\frac{\mathrm{d}|\Gamma^B(s_{-+})|^2}{\mathrm{d}y}\right)^2\right]} \tag{2.32}$$

which quantifies the statistical sensitivity for a given binning, relative to the one achievable in an unbinned analysis. The CLEO collaboration defined an *optimal* binning scheme by an iterative procedure where, starting from the equal binning scheme, a micro-bin is randomly reassigned new bin numbers in each step, and a step accepted if Q^2 increases. The optimisation is done for the case where $x = y = 0$ and thus Q^2 simplifies to $Q^2_{x=y=0} = \sum_i N_i^{x=y=0}(c_i^2 + s_i^2)/N_{total}^{x=y=0})$. The resulting binning scheme is shown in Fig. **??**. An additional binning scheme is defined, denoted the *modified optimal* scheme and shown in Fig. **??**, where the Q^2 figure of merit is modified to take into account the presence of backgrounds []. The modified optimal binning scheme has proven beneficial to use in measurements with small signal yields [], but is not employed in the present thesis.

While the *definition* and *optimisation* of these binning schemes depend on knowledge of $A_{\mathrm{S}}^D(s_-, s_+)$ via an amplitude model, it is important to note that no model information is used when the binning schemes are used in the subsequent measurements of strong-phases[5] or *CP*-observables. Therefore the measurements will not be biased by any modelling imperfections, although the obtained precision might be lower than expected.

Both the CLEO and BESIII collaborations have measured the values of c_i and s_i for the equal, optimal, and modified optimal binning schemes. The results are shown in Figs. **??** and **??**, where they are also compared to the expectation from the latest amplitude model. The measurements presented in this thesis are based on a combination of the BESIII and CLEO results for the optimal binning scheme, made by the BESIII collaboration [], and tabulated in Table **??**.

The preceding discussion has been focusing on the $D \to K^0_{\mathrm{S}}\pi^+\pi^-$ channel, however the $D \to K^0_{\mathrm{S}}K^+K^-$ channel can be analysed in completely analogously.

[5]With the exception of minimal model-dependence introduced when the $K^0_{\mathrm{L}}\pi^+\pi^-$ final state is employed to constrain the s_i parameters by the D-factories [], the impact of which is well under control.

The CLEO collaboration measure c_i and s_i values for this mode as well, in three binning schemes. These are all equal-phase binning schemes, with 2, 3, and 4 bins, respectively, shown in Fig. **??**. The $D \to K^0_S K^+ K^-$ decay amplitude is almost completely dominated by two K^+K^- resonances, the *CP*-odd $\phi(1020)$ and the *CP*-even $a_0(980)$, and this means that very little gain in sensitivity can be made by altering the equal-phase binning schemes. The measured c_i and s_i values are shown in Fig. **??** and tabulated in Table **??**. A BESIII measurement is in preparation, but has not been finished at the time of writing.

2.3.5 Global CP asymmetry and the relation to GLW and ADS measurements

The introduction of separate normalisation factors h^+ and h^- in Eq. (2.25) hides the fact that information on γ (in principle) can be obtained from the asymmetry in phase-space-integrated B^+ and B^- yields. In the ideal case where $h^- = h^+$ the total yield asymmetry is

$$\begin{aligned} A_{GGSZ} &= \frac{\sum_i N^-_- - N^+_i}{\sum_{i=-N}^{N} N^- i - + N^+_i} = \frac{\sum_{i=-N}^{N} \sqrt{K_i K_{-i}} c_i (x_- - x_+)}{1 + r_B^2 + 2\sum_{i=-N}^{N} \sqrt{K_i K_{-i}} c_i (x_- + x_+)} \\ &= \frac{2\sum_{i=1}^{N} \sqrt{K_i K_{-i}} c_i (x_- - x_+)}{1 + r_B^2 + 4\sum_{i=1}^{N} \sqrt{K_i K_{-i}} c_i (x_- + x_+)}, \end{aligned} \tag{2.33}$$

where it has been exploited that $\sum_{i=-N}^{N} \sqrt{K_i K_{-i}} s_i = 0$ by definition. The size of the asymmetry is governed by the factor $\sum_{i=1}^{N} \sqrt{K_i K_{-i}} c_i$, which is small for $D \to K^0_S \pi^+ \pi^-$ and $D \to K^0_S K^+ K^-$ decays. The underlying reason is that $\delta_D(s_-, s_+)$ varies significantly across phase-space for these decays, as evident by the spread in the values of c_i in Tables **??** and **??**, which reduces the *average* of the asymmetry-generating D^0–$\overline{D}^0$ interference term to being close to zero. As such, the value of $\sum_{i=-N}^{N} \sqrt{K_i K_{-i}} c_i$ is closely related to the *CP* content of the final state in question: for a self-conjugate *CP* even (odd) final state it is true that

$$A_{D^0}(s_-, s_+) = {}^{+}_{(-)} A_{\overline{D}^0}(s_-, s_+) = {}^{+}_{(-)} A_{D^0}(s_+, s_-) \tag{2.34}$$

and thus $\sum_{i=1}^{N} \sqrt{K_i K_{-i}} c_i = {}^{+}_{(-)} 1$. This motivates the definition of the *CP*-even fraction of the decay

$$\mathcal{F}_+ \equiv \frac{1}{2}\left(1 + \sum_{i=1}^{N} \sqrt{K_i K_{-i}} c_i\right). \tag{2.35}$$

With $\mathcal{F}_+$ in hand, the asymmetry in Eq. (2.33) can be rewritten

$$A_{GGSZ} = \frac{(2\mathcal{F}_+ - 1) r_B \sin\delta_B \sin\gamma}{1 + r_B^2 (2\mathcal{F}_+ - 1) 2 r_B \cos\delta_B \cos\gamma}, \tag{2.36}$$

which is the usual form used in quasi-GLW measurements []; for $N = 1$ the definition in Eq. (2.35) is equivalent to $\mathcal{F}_+$ as defined in Ref. []. From the definition of K_i and c_i it follows that the value of $\mathcal{F}_+$ is independent of the number and shape of bins in a given binning scheme, as long as the bin definitions follow the symmetry principles outlined in Section **??**. For $D \to K^0_S\pi^+\pi^-$ and $D \to K^0_S K^+K^-$ decays the values of $\mathcal{F}_+$ are

$$\begin{aligned} \mathcal{F}_+(K^0_S\pi^+\pi^-) &= X? \\ \mathcal{F}_+(K^0_S K^+K^-) &= X? \end{aligned} \tag{2.37}$$

as evaluated with the Belle 2018 model for $D \to K^0_S\pi^+\pi^-$ decays and the BaBar 2010 model for $D \to K^0_S K^+K^-$ decays. Since $r_B^{DK^\pm} \sim 0.1$ the predicted global asymmetries are thus approximately 1–2 %, which is not resolvable with the current experimental yields. As shown in Chapter 4, *CP* violation in the K^0_S sector leads to asymmetries of a similar size, further complicating the use of global asymmetries to constrain $x_\pm$ and $y_\pm$. Thus these modes are ill-suited for quasi-GLW measurements, and ignoring global asymmetries leads to a negligible loss of information on γ. The reverse is true for a well-suited quasi-GLW mode, such as $D \to \pi^+\pi^-\pi^0$: if $\mathcal{F}_+$ is close to either zero or unity, it means that (c_i, s_i) will be close to $(\pm 1, 0)$ in all bins for *any* given binning scheme, and the set of bins will provide almost identical constraints on $x_\pm$ and $y_\pm$. Thus, the binning of phase space leads to no gain in precision compared to a global analysis.

Indeed, a crucial quality of the GGSZ method, is that exactly because each bin-pair provides independent constraints on $x_\pm$ and $y_\pm$, the method provides a single solution for (γ, r_B, δ_B) that does not suffer the ambiguities of the ADS and GLW approaches. In order to illustrate this further, it is useful to make one more comparison of the model-independent GGSZ formalism to the ADS and GLW formalisms. If there was no *CP* symmetry the B^+ yield in bin $+i$ would equal the B^- yield in bin $-i$. Therefore the relevant *CP* asymmetry for a given Dalitz bin is

$$\begin{aligned} A^i_{GGSZ} &\equiv \frac{N^-_i - N^+_{-i}}{N^-_i + N^+_{-i}} \\ &= \frac{\sqrt{K_i K_{-i}}(c_i(x_- - x_+) + s_i(y_- - y_+))}{K_i + r_B^2 K_{-i} + 2\sqrt{K_i K_{-i}}(c_i(x_- + x_+) + s_i(y_- + y_+))}. \end{aligned} \tag{2.38}$$

This expression is identical to the ADS asymmetry in Eq. (**??**) if the effective D-decay parameters r^i_D and δ^i_D are defined via

$$\kappa_i \cos\delta^i_D \equiv c_i \quad , \quad \kappa_i \sin\delta^i_D \equiv s_i \quad , \quad r^i_D \equiv \sqrt{K_i/K_{-i}}, \tag{2.39}$$

Table 2.1: Classification of the bins used in model-independent GGSZ measurements, in terms of whether the interplay between the D^0 and $\overline{D}^0$ amplitudes in the bin resemble typical GLW or ADS behaviour. The parameters are calculated using the 2018 Belle model [] for $D \to K^0_S\pi^+\pi^-$ decays and the 2010 BaBar model [] for $D \to K^0_S K^+K^-$ decays.

Optimal binning scheme: $D \to K^0_S\pi^+\pi^-$					
Bin i	$\hat{r}_D$	$\hat{\delta}_D$	$\mathcal{F}_+$	κ	Bin type
1	0.473	91.9°	48.97 %	0.81	Mixed
2	0.164	11.1°	63.38 %	0.85	ADS-like
3	0.157	79.4°	52.50 %	0.89	ADS-like
4	0.768	175.3°	5.85 %	0.92	GLW-odd-like
5	0.759	−99.9°	42.84 %	0.87	Mixed
6	0.223	−64.5°	57.92 %	0.87	ADS-like
7	0.651	−13.3°	89.44 %	0.89	GLW-even-like
8	1.745	21.0°	87.08 %	0.92	GLW-even-like

2-bins binning scheme: $D \to K^0_S K^+K^-$					
Bin i	$\hat{r}_D$	$\hat{\delta}_D$	$\mathcal{F}_+$	κ	Bin type
1	0.816	19.8°	86.14 %	0.78	GLW-even-like
2	0.775	154.5°	16.23 %	0.77	GLW-odd-like

and a coherence factor, κ, is included in the interference terms of the ADS expression, as is standard for multi-body D decays []. These parameters allow us to classify a given pair of bins with number $\pm i$ as either *GLW-like*, if δ^i_D is close to 0 or π and r^i_D is close to unity, or *ADS-like* if $0 < r^i_D \ll 1$. The *CP*-even fraction of the D-decay can also be defined for a given bin-pair:

$$\mathcal{F}^i_+ = \mathcal{F}^{-i}_+ \equiv \frac{1}{2}\left(1 + 2c_i\frac{\sqrt{K_i K_{-i}}}{K_i + K_{-i}}\right) = \frac{1}{2}\left(1 + 2c_i\frac{r^i_D}{1 + {r^i_D}^2}\right). \tag{2.40}$$

A GLW-even-like bin pair will have $\mathcal{F}^i_+ \simeq 1$ and a GLW-even-like bin pair will have $\mathcal{F}^i_+ \simeq -1$.

Table 2.1 summarises a classification of the bins for the optimal $D \to K^0_S\pi^+\pi^-$ binning scheme and the 2-bins $D \to K^0_S K^+K^-$ binning scheme following these principles. Two bins are classified as *mixed* because r^i_D is not particularly small, but $\mathcal{F}^i_+$ is close to 0.5. The fact that multiple bin types appear for both the $D \to K^0_S\pi^+\pi^-$ and $D \to K^0_S K^+K^-$ modes underline that each mode benefits from being analysed in the GGSZ formalism, and that the bins provide independent constraints that allows for a single, non-ambiguous solution for (γ, r_B, δ_B).

2.4 Strategy for the LHCb measurement

The main topic of this thesis is a model-independent GGSZ measurement using $B^\pm \to DK^\pm$ and $B^\pm \to D\pi^\pm$ decays, and the two D final states $K^0_S\pi^+\pi^-$ and $K^0_S K^+K^-$. The measurement uses the optimal binning scheme for the $D \to K^0_S\pi^+\pi^-$ mode, with the combined strong-phase inputs from the BESIII [] and CLEO [] collaborations published in Ref. []. For the $D \to K^0_S K^+K^-$ channel, the 2-bins scheme is used with the strong-phase parameters measured by the CLEO collaboration []. The details of the analysis are presented in Chapter (5), but the overall strategy and a few extensions of the formalism from the previous sections are given here.

Due to the geometry of the LHCb detector, the signal reconstruction efficiency for $B^\pm \to D(\to K^0_S h^+h^-)h'^\pm$ decays varies significantly across the D-decay phase space. Denoting the efficiency profile as $\eta(s_-, s_+)$, the yield equations of Eq. (2.25) are therefore modified slightly

$$\begin{aligned} N_i^- &= h^{B^-}\left[F_i + r_B^2 F_{-i} + 2\sqrt{F_i F_{-i}}\,(c'_i x_- + s'_i y_-)\right], \\ N_i^+ &= h^{B^+}\left[F_{-i} + r_B^2 F_i + 2\sqrt{F_i F_{-i}}\,(c'_i x_+ - s'_i y_+)\right], \end{aligned} \tag{2.41}$$

where the phase-space integrated quantities now include the efficiency profile

$$F_i = \frac{1}{N_F}\int_i \mathrm{d}s^2\,\eta(s_{-+})|A^D_S(s_{-+})|^2, \qquad N_F = \int \mathrm{d}s^2\,\eta(s_{-+})|A^D_S(s_{-+})|^2, \tag{2.42}$$

$$c'_i = \frac{\int_i \mathrm{d}s^2\,\eta(s_{-+})|A^D_S(s_{-+})||A^D_S(s_{+-})|\cos[\delta_D(s_{-+})]}{\sqrt{\int_i \mathrm{d}s^2\,\eta(s_{-+})|A^D_S(s_{-+})|^2}\sqrt{\int_i \mathrm{d}s^2\,\eta(s_{-+})|A^D_S(s_{+-})|^2}}, \tag{2.43}$$

with an analogous definition of s'_i. At leading order, the strong-phase parameters are unaffected by the non-uniform efficiency, and, in addition, the bin definitions favour bins for which c_i and s_i take on similar values across each bin. Therefore, the reported c_i and s_i values are used directly in the measurement. The impact on the obtained central values is negligible, as described in detail in Section **??** where a systematic uncertainty is assigned.

The F_i *are* significantly different to the K_i due to the experimental acceptance profile in LHCb. Given external inputs for the strong-phase parameters, it is possible to fit the F_i parameters *and* $x_\pm$ and $y_\pm$ simultaneously in a fit to the LHCb $B^\pm \to DK^\pm$ data set, in which case the obtained F_i parameters incorporate the correct acceptance profile correction by construction. However, the obtainable precision for the *CP* observables measured by this procedure is suboptimal.

As an alternative, the first LHCb measurement made a simultaneous analysis of $B^\pm \to DK^\pm$ and a much larger sample of $B^\pm \to D\pi^\pm$ decays; since the F_i parameters relate to the D decay, they can effectively be obtained in the $D\pi^\pm$ sample and shared between the two $B^\pm \to Dh^\pm$ channels. However, there is *CP* violation present in the $B^\pm \to D\pi^\pm$ decays, which led to a dominant systematic uncertainty. Later LHCb measurements instead relied on flavour tagged D mesons from $\overline{B}^0 \to D^{*+}(\to D^0\pi^+)\mu^-\bar{\nu}_\mu X$ decays, where no *CP* violation in possible, to obtain F_i. However, due to necessarily different triggering paths and selections, the acceptance profile is not exactly identical between semi-leptonic decays and the $B^\pm \to Dh^\pm$ decays of interest. An efficiency correction based on simulation was therefore applied to obtain the correct F_i; the uncertainty related to the correction constituted the largest systematic uncertainty to the measurement [].

Both sources of systematic uncertainty can be avoided by making a simultaneous analysis of $B^\pm \to DK^\pm$ and $B^\pm \to D\pi^\pm$ decays, where *CP*-violating observables are measured in *both* channels and the F_i parameters are shared. Effectively, the F_i are determined in the high statistics $B^\pm \to D\pi^\pm$ channel, but with no systematic effect from *CP*-violation in that channel, since the *CP*-violation is incorporated in the yield description. At the start of the work that lead to this thesis, it was not clear to what degree the measured *CP*-violating observables in $B^\pm \to D\pi^\pm$ decays were affected by *CP* violation in the neutral kaon sector. The impact had been shown to scale as $\mathcal{O}(|\epsilon|/r_B)$ [], which is negligible for the $B^\pm \to DK^\pm$ channel but suggests potentially large biases in the $B^\pm \to D\pi^\pm$ channel, where r_B is 20 times smaller. However, the dedicated analysis presented in Chapter 4 has proved the effect on GGSZ measurements to be in fact be *smaller* than $\mathcal{O}(|\epsilon|/r_B)$ and the simultaneous measurement is indeed viable.

The measurement is performed, by making extended maximum-likelihood fits to the m_B spectra of $B \to D(\to K^0_S h^+h^-)K^\pm$ candidates split by charge and Dalitz bin, where the signal yields are parameterised using the expressions in Eq. (**??**), thus obtaining values for $x_\pm^{DK}$ and $y_\pm^{DK}$ directly. The Cartesian *CP*-violating observables $x_\pm$ and $y_\pm$ are employed because they lead to better statistical behaviour than fits to data where the underlying parameters $(\gamma, r_B^{DK^\pm}, \delta_B^{DK^\pm})$ are determined [], at the cost of introducing a fourth degree of freedom.

With the addition of the $B^\pm \to D\pi^\pm$ mode as a true signal channel, two new underlying parameters are introduced, $r_B^{D\pi^\pm}$ and $\delta_B^{D\pi^\pm}$. It is only necessary to introduce an additional two, not four, Cartesian parameters [] by defining

$$\xi_{D\pi^\pm} = \left(\frac{r_B^{D\pi^\pm}}{r_B^{DK^\pm}}\right) \exp[i(\delta_B^{D\pi^\pm} - \delta_B^{DK^\pm})] \tag{2.44a}$$

and letting

$$x_{\xi}^{D\pi} = \mathrm{Re}[\xi_{D\pi^{\pm}}] \qquad\qquad y_{\xi}^{D\pi} = \mathrm{Im}[\xi_{D\pi^{\pm}}]. \tag{2.44b}$$

In terms of these parameters, the usual Cartesian $x_{\pm}$ and $y_{\pm}$ are given by

$$x_{\pm}^{D\pi} = x_{\xi}^{D\pi} x_{\pm}^{DK} - y_{\xi}^{D\pi} y_{\pm}^{DK}, \qquad y_{\pm}^{D\pi} = x_{\xi}^{D\pi} y_{\pm}^{DK} + y_{\xi}^{D\pi} x_{\pm}^{DK}. \tag{2.45}$$

Using this expression, the $B^{\pm} \to D\pi^{\pm}$ yields can also be defined via Eq. (**??**) in the maximum-likelihood fit. This allows for a stable fit for all six x and y parameters, as well as the shared F_i, as described in much greater detail in Chapter **??**. Note that ξ does not depend on γ: all information on *CP* asymmetries in both the $B^{\pm} \to DK^{\pm}$ and $B^{\pm} \to D\pi^{\pm}$ channels is encoded in $x_{\pm}^{DK}$ and $y_{\pm}^{DK}$.

The combined analysis of $B^{\pm} \to DK^{\pm}$ and $B^{\pm} \to D\pi^{\pm}$ decays presents a significant step forward, because it solves the problem of obtaining F_i parameters for the appropriate acceptance profile in a manner that avoids leading systematic uncertainties, and almost all reliance on simulation. This is of great importance, if the large data samples that will be collected by LHCb in the future are to be exploited to their full potential.

3
The LHCb experiment

We have a detector? I thought ntuples were made of magic.

3.1 Subdetectors

3.1.1 The VELO

3.1.2 Magnet and tracking stations

3.1.3 The RICH

3.1.4 Calorimeters

3.1.5 Muon detectors

3.2 Track reconstruction

3.3 The LHCb triggerring system

3.3.1 The level-0 hardware trigger

3.3.2 High-level triggers

3.3.3 Offline data filtering: the LHCb stripping

3.4 Simulation

4

Neutral kaon CP violation and material interaction in GGSZ measurements

- EVERYTHING is based on an effective Hamiltonian approach cf the PDG CPV review. That's fine but do mention conditions: we only care about the $K^0_{\rm S}$ and $K^0_{\rm L}$ wavefunctiong components, and for times faster than the strong interaction times

Let's see how much I can get away with simply copying from the paper. Large amounts of the initial theory can be moved to the theory chapter of course.

4.1 CP violation and material interaction of neutral kaons

We will extend an earlier definition slightly, and let

$$A^{(\overline{D})}_{\rm S(L)}(s_-, s_+) = A(\,^{(}\overline{D}^{)0} \to K^0_{\rm S(L)}\pi^+\pi^-). \tag{4.1}$$

The derivation in the preceding section assumed that $K^0_{\rm S}$ is a *CP* eigenstate, however this is known to be an approximation. Including *CP* violation in the neutral kaons, the mass eigenstates $K^0_{\rm S}$ and $K^0_{\rm L}$ are given by

$$|K^0_{\rm S}\rangle = \frac{1}{\sqrt{1+|\epsilon|^2}}\left[|K_1\rangle + \epsilon|K_2\rangle\right], \qquad |K^0_{\rm L}\rangle = \frac{1}{\sqrt{1+|\epsilon|^2}}\left[|K_2\rangle + \epsilon|K_1\rangle\right], \tag{4.2}$$

in terms of the *CP* even (odd) eigenstates $K_{1(2)} = (K^0 + (-)\overline{K}^0)/\sqrt{2}$ and the *CP* violation parameter $\epsilon = A(K^0_{\rm L} \to \pi^+\pi^-)/A(K^0_{\rm S} \to \pi^+\pi^-)$, measured to be [**?**]

$$|\epsilon| = (2.228 \pm 0.011) \times 10^{-3}, \qquad \arg\epsilon = (43.52 \pm 0.05)^\circ. \tag{4.3}$$

The phase-convention $\hat{C}\hat{P}|K^0\rangle = |\overline{K}^0\rangle$ is used and direct *CP* violation in the kaon decay is ignored, as the effect is three orders of magnitude smaller than indirect *CP* violation [**?**]. The non-zero amplitude for the $K^0_{\rm L} \to \pi^+\pi^-$ decay introduces a direct dependence on the $A_{\rm L}^{(\overline{D})}$ amplitudes. Whereas Eq. (2.24a) assumed that $\mathrm{d}\Gamma^-(t, s_{-+}) \propto \left|\psi^-_{\rm S}(t, s_{-+})\right|^2$, the actual decay rate satisfies

$$\mathrm{d}\Gamma^-(t, s_{-+}) \propto \left|\psi^-_{\rm S}(t, s_{-+}) + \epsilon\psi^-_{\rm L}(t, s_{-+})\right|^2, \tag{4.4}$$

where $\psi^-_{\rm S}$ and $\psi^-_{\rm L}$ are the $K^0_{\rm S}$ and $K^0_{\rm L}$ components of the neutral kaon state.[1] The $A_{\rm L}^{(\overline{D})}$ amplitudes do not satisfy Eq. (2.22), but instead $A^D_{\rm L}(s_{-+}) \simeq -A^{\overline{D}}_{\rm L}(s_{+-})$, and therefore the presence of the $K^0_{\rm L}$ term leads to corrections to the yield expressions in Eq. (**??**). In an experimental setting, the dependence on the $A_{\rm L}^{(\overline{D})}$ amplitudes is further enhanced by material interactions of the neutral kaon, because different nuclear interaction strengths of the K^0 and $\overline{K}^0$ mesons introduce a non-zero $K^0_{\rm S} \leftrightarrow K^0_{\rm L}$ transition amplitude for neutral kaons traversing a detector segment. This effect was predicted early in the history of kaon physics [**?**] and is commonly denoted *kaon regeneration*. The general expression for the time dependent neutral kaon state components is [**?**, **?**]

$$\begin{aligned}
\psi_{\rm S}(t, s_{-+}) &= e^{-i\Sigma t}\left(\psi^0_{\rm S}(s_{-+})\cos\Omega t + \frac{i}{2\Omega}\left(\Delta\lambda\psi^0_{\rm S}(s_{-+}) - \Delta\chi\psi^0_{\rm L}(s_{-+})\right)\sin\Omega t\right), \\
\psi_{\rm L}(t, s_{-+}) &= e^{-i\Sigma t}\left(\psi^0_{\rm L}(s_{-+})\cos\Omega t - \frac{i}{2\Omega}\left(\Delta\lambda\psi^0_{\rm L}(s_{-+}) + \Delta\chi\psi^0_{\rm S}(s_{-+})\right)\sin\Omega t\right),
\end{aligned} \tag{4.5}$$

in terms of the parameters

$$\begin{aligned}
\Delta\chi &= \chi - \bar{\chi}, \\
\Delta\lambda &= \lambda_{\rm L} - \lambda_{\rm S} = (m_{\rm L} - m_{\rm S}) - \frac{i}{2}(\Gamma_{\rm L} - \Gamma_{\rm S}), \\
\Sigma &= \frac{1}{2}\left(\lambda_{\rm S} + \lambda_{\rm L} + \chi + \bar{\chi}\right), \\
\Omega &= \frac{1}{2}\sqrt{\Delta\lambda^2 + \Delta\chi^2},
\end{aligned} \tag{4.6}$$

where $m_{\rm S(L)}$ and $\Gamma_{\rm S(L)}$ are the mass and decay width of the $K^0_{\rm S}$ ($K^0_{\rm L}$) mass eigenstates, and the parameters χ and $\bar{\chi}$ describe the material interaction of the K^0 and $\overline{K}^0$

[1] The time dependence of Eq. (4.4) is kept implicit in Eq. (2.24a), as it contributes a factor that is constant over phase-space in the $\epsilon = 0$ approximation.

flavour eigenstates. The χ ($\bar{\chi}$) parameter is proportional to the forward scattering amplitude of a K^0 ($\overline{K}^0$) meson in a traversed material. In Eq. (4.5), $\psi^0_{\rm S}$ and $\psi^0_{\rm L}$ are the initial $K^0_{\rm S}$ and $K^0_{\rm L}$ components of the neutral kaon state, which depend on the phase-space coordinates of the D decay: $\psi^0_{\rm S/L} \propto \mathcal{A}_{\rm S/L}(s_{-+})$. Thus, for $\Delta\chi \neq 0$, $\psi_{\rm S}(t)$ depends on $\mathcal{A}_{\rm L}(s_{+-})$ irrespective of the $K^0_{\rm L} \to \pi^+\pi^-$ decay, due to kaon regeneration.

In addition, the relations $A^{\overline{D}}_{\rm S}(s_{-+}) = A^D_{\rm S}(s_{+-})$ and $A^{\overline{D}}_{\rm L}(s_{-+}) = -A^D_{\rm L}(s_{+-})$ are not exact for $\epsilon \neq 0$, as $K^0_{\rm S}$ and $K^0_{\rm L}$ are not exact CP eigenstates. This leads to further corrections to the yield expressions in Eq. (**??**). It it beneficial to express $A^D_{\rm S(L)}$ in terms of the amplitudes $A^D_{1(2)}$, defined analogously to Eq. (2.21) but for the CP even (odd) eigenstates K_1 (K_2). After the decay of a D^0 meson to a neutral kaon, the kaon state is

$$\begin{aligned}\psi^0 &= A^D_1|K_1\rangle + A^D_2|K_2\rangle \\ &= N\left[(A^D_1 - \epsilon A^D_2)|K^0_{\rm S}\rangle + (A^D_2 - \epsilon A^D_1)|K^0_{\rm L}\rangle\right],\end{aligned} \tag{4.7}$$

with the normalisation constant $N = \sqrt{1+|\epsilon|^2}/(1-\epsilon^2)$. Thus it can be seen that

$$\begin{aligned}A^D_{\rm S}(s_{+-}) &= N\left[(A^D_1(s_{+-}) - \epsilon A^D_2(s_{+-}))\right], \\ A^D_{\rm L}(s_{+-}) &= N\left[(A^D_2(s_{+-}) - \epsilon A^D_1(s_{+-}))\right],\end{aligned} \tag{4.8}$$

with an analogous expression for the $\overline{D}^0$ decay amplitudes. Therefore, the generalised relations between the D^0 and $\overline{D}^0$ amplitudes are

$$\begin{aligned}A^{\overline{D}}_{\rm S}(s_{+-}) = &\quad N[A^{\overline{D}}_1(s_{+-}) - \epsilon A^{\overline{D}}_2(s_{+-})] \\ = &\quad N[A^D_1(s_{-+}) + \epsilon A^D_2(s_{-+})] = \quad A^D_{\rm S}(s_{-+}) + 2N\epsilon A^D_2(s_{-+}), \\ A^{\overline{D}}_{\rm L}(s_{+-}) = &\quad N[A^{\overline{D}}_2(s_{+-}) - \epsilon A^{\overline{D}}_1(s_{+-})] \\ = &-N[A^D_2(s_{-+}) + \epsilon A^D_1(s_{-+})] = -A^D_{\rm L}(s_{-+}) - 2N\epsilon A^D_1(s_{-+}).\end{aligned} \tag{4.9}$$

In order to calculate the full corrections to the yield expressions in Eq. (**??**), models of $A^D_{\rm S}$ and $A^D_{\rm L}$ (or A^D_1 and A^D_2) are needed. While there are several amplitude models available to describe the decay amplitude $A(D^0 \to K^0_{\rm S}\pi^+\pi^-)$ [**?**, **?**, **?**, **?**, **?**], no models have been published for $D^0 \to K^0_{\rm L}\pi^+\pi^-$ decays. However, following the assumptions laid out in Ref. [**?**], the amplitudes $A^D_1(s_{+-})$ and $A^D_2(s_{+-})$ can be related, allowing both qualitative and quantitative estimates of the bias effects to be made with existing $D^0 \to K^0_{\rm S}\pi^+\pi^-$ models. In the isobar formalism, the decay amplitude $A(D^0 \to K_1\pi^+\pi^-)$ is expressed as a non-resonant constant amplitude plus a sum of resonances

$$A(D^0 \to K_1\pi^+\pi^-) = k_{NR} + \sum_{CF} k_i R^i(s_{K\pi^-}) + \sum_{DCS} k_j R^j(s_{K\pi^+}) + \sum_{R_{\pi\pi}} k_k R^k(s_{\pi^+\pi^-}). \tag{4.10}$$

The resonances are split into Cabibbo-favoured (CF) K^{*-} resonances, doubly Cabibbo-suppressed (DCS) K^{*+} resonances and $\pi\pi$ resonances. The R functions are taken to describe all kinematical dependence and are well described in eg. Refs. [**?**, **?**] and references therein. In modern models, the $\pi\pi$ and $K\pi$ S-wave components are modelled via the K-matrix formalism and LASS parametrisations, respectively, instead of sums of individual resonances [**?**]. This does not alter the arguments below, as the R functions of Eq. (4.10) can equally well represent such terms. The CF resonances couple to the $\overline{K}^0$ component of $K_1(\propto K^0 + \overline{K}^0)$, and therefore the corresponding k_i in the $K_2(\propto K^0 - \overline{K}^0)$ amplitude will have a relative minus sign. The DCS resonances couple to the K^0 component of K_1, and so the corresponding k_j in the K_2 amplitude will have a relative plus sign. For the h^+h^- resonances, there will be a coupling to both the K^0 and $\overline{K}^0$ components, however the coupling to the K^0 component is expected to be suppressed with a Cabibbo suppression factor $r_k e^{i\delta_k}$, where $r_k \simeq \tan^2\theta_C \simeq 0.05$ is determined by the Cabibbo angle θ_C and δ_k can take any value. Therefore, the k_k for these resonances have a relative $-(1 - 2r_k e^{i\delta_k})$ factor in the K_2 amplitude. The same effect leads to the differences in decay rates between $D^0 \to K^0_S\pi^0$ and $D^0 \to K^0_L\pi^0$ decays [**?**, **?**]. An important consequence of these substitution rules is that

$$A_2^D(s_{+-}) = -A_1^D(s_{+-}) + r_A \Delta A(s_{+-}), \tag{4.11}$$

where $r_A \simeq \tan^2\theta_C$ and $\Delta A(s_{+-}) \sim A_1^D(s_{+-})$ are of the same order of magnitude (at least when averaged over the bins used in γ measurements). This relation is sufficient to make the qualitative arguments of Section **??**, while the full set of substitution rules above are used in the quantitative studies of Section **??**.

4.1.1 Impact on γ measurements: principles

With suitable models to calculate $A^{(\overline{D})}_{S(L)}$ (or $A^{(\overline{D})}_{1/2}$) and knowledge of $\Delta\chi$ for the materials relevant to an experimental setting, Eqs. (4.4), (4.5), and (4.9) can be integrated to calculate the expected phase-space bin yields, $N_i^{\pm}$, including the effects of kaon *CP* violation and material interaction. Preliminary to doing this in Section **??**, it is useful to look at the lowest order corrections to Eq. (**??**) in ϵ and $r_\chi = \frac{1}{2}\frac{\Delta\chi}{\Delta\lambda}$, the dimensionless parameter governing material interactions. For LHCb and Belle II the average $|r_\chi| \simeq 10^{-3}$, as detailed in the Section **??**. The studies of this section are made with the assumption of a flat phase-space efficiency and

uniform acceptance over all decay times. Time-acceptance effects will be treated in Section **??**. To first order in r_χ, the expression in Eq. (4.5) simplifies to [**?**]

$$\begin{aligned}\psi_{\rm S}(t,s_{+-}) &= e^{-\frac{i}{2}(\chi+\bar{\chi})t}e^{-i\lambda_{\rm S}t}\left(\psi^0_{\rm S}(s_{+-}) - r_\chi\left(1-e^{-i\Delta\lambda t}\right)\psi^0_{\rm L}(s_{+-})\right),\\ \psi_{\rm L}(t,s_{+-}) &= e^{-\frac{i}{2}(\chi+\bar{\chi})t}e^{-i\lambda_{\rm L}t}\left(\psi^0_{\rm L}(s_{+-}) + r_\chi\left(1-e^{+i\Delta\lambda t}\right)\psi^0_{\rm S}(s_{+-})\right).\end{aligned} \tag{4.12}$$

In model-independent measurements, the K_i are obtained in a data-driven way using flavour-tagged D samples, and by averaging over D^0 and $\overline{D}^0$ decays. Therefore it proves beneficial to introduce the parameters

$$\hat{K}_i = \frac{1}{1+|\epsilon+r_\chi|^2\frac{\Gamma_{\rm S}}{\Gamma_{\rm L}}}\left(K_i^{(1)} + |\epsilon+r_\chi|^2\frac{\Gamma_{\rm S}}{\Gamma_{\rm L}}K_i^{(2)}\right), \tag{4.13}$$

in which the $K_i^{(1/2)}$ parameters are phase-space integrals, defined as in Eq. (2.27) but for $A^D_{1/2}$. The $\hat{K}_i$ correspond to the expected measured value of $K_i^{\rm meas} = (N_i^D + N_{-i}^{\overline{D}})/(\sum_j N_j^D + N_{-j}^{\overline{D}})$ to lowest order in ϵ and r_χ, where N_i^D ($N_i^{\overline{D}}$) is the expected yield of flavour tagged D^0 ($\overline{D}^0$) mesons into bin i of the D decay phase-space. In fits of amplitude models where both flavour tagged D^0 and $\overline{D}^0$ decays are used to fit the $D\to K^0_{\rm S}\pi^+\pi^-$ amplitude, related via Eq. (2.22), one will effectively fit an amplitude describing $N_i^D + N_{-i}^{\overline{D}}$, and therefore the arguments below, based on $\hat{K}_i$, will also hold for model-dependent measurements. Employing Eq. (4.11) in Eq. (4.13), the expected yields can be written

$$\begin{aligned}N_i^- &= h_B^{-'}\left(\hat{K}_{+i} + r_B^2\hat{K}_{-i} + 2\sqrt{\hat{K}_{+i}\hat{K}_{-i}}(x_-\hat{c}_i + y_-\hat{s}_i) + O(r\epsilon)\right),\\ N_i^+ &= h_B^{+'}\left(\hat{K}_{-i} + r_B^2\hat{K}_{+i} + 2\sqrt{\hat{K}_{+i}\hat{K}_{-i}}(x_+\hat{c}_i - y_+\hat{s}_i) + O(r\epsilon)\right),\end{aligned} \tag{4.14}$$

where $O(r\epsilon)$ denotes terms of $O(r_A\epsilon)$, $O(r_B\epsilon)$, $O(r_Ar_\chi)$, and $O(r_Br_\chi)$. Since $r_B\sim r_A\sim 10^{-1}$ (in $B^\pm\to DK^\pm$ decays) and $r_\chi\sim\epsilon\sim 10^{-3}$, these terms are all of the same order of magnitude. The new normalisation constants $h_B^{\pm'} = h_B^\pm(1 + |\epsilon+r_\chi|^2\frac{\Gamma_{\rm S}}{\Gamma_{\rm L}} \mp \Delta h)$ are defined in terms of

$$\Delta h = 2{\rm Re}[\epsilon+r_\chi] - 4\frac{\Gamma_{\rm S}}{\Gamma_{\rm L}+\Gamma_{\rm S}}\frac{{\rm Re}[\epsilon+r_\chi]+\mu{\rm Im}[\epsilon+r_\chi]}{1+\mu^2},\quad \mu = 2\frac{m_{\rm L}-m_{\rm S}}{\Gamma_{\rm L}+\Gamma_{\rm S}}. \tag{4.15}$$

The parameters $(\hat{c}_i,\hat{s}_i)$ have been introduced to denote the *measured* average strong-phases, which are expected to differ from (c_i,s_i) at $O(\epsilon)$, since neutral kaon *CP* violation is not taken into account in the measurements by CLEO. The corrections are thus in the neglected $O(r_B\epsilon)$ terms.

Two observations can be made from the expression in (4.14). The first is that the phase-space *distribution* is only changed at $O(r\epsilon)$ compared to the expression

in Eq. (**??**), if the measured $\hat{K}_i$ are used in the experimental analysis. As the $D^0 - \overline{D}^0$ interference term that provides sensitivity to γ enters at order $O(r_B)$, the impact on γ measurements can be expected to be $\Delta\gamma/\gamma \sim O(r\epsilon/r_B)$. For $B \to DK$ analyses, where $r_B \simeq 0.1$, this is at the permille level, so the induced $\Delta\gamma$ bias can be expected to be smaller than 1°. This holds true, unless the integrated material interaction, and thereby effective r_χ, varies significantly across the D-decay phase-space due to experimental effects. However, this is unlikely to be the case in practice, since no significant correlation between the phase-space coordinates and the travel direction of the kaon is expected.

The second observation relates to potential future measurements of γ, which may also include sensitivity from the total, phase-space-integrated yield asymmetry

$$A_{\text{total}} = \frac{N^- - N^+}{N^- + N^+} = \frac{2\sum_i c_i\sqrt{\hat{K}_i\hat{K}_{-i}}r_B \sin\delta_B \sin\gamma + \Delta h}{1 + r_B^2 + 2\sum_i c_i\sqrt{\hat{K}_i\hat{K}_{-i}}r_B \cos\delta_B \cos\gamma} + O(r\epsilon), \qquad (4.16)$$

which was considered in Ref. [**?**]. In the limit $r_B \to 0$ the expression agrees with the result for the analogous asymmetry in $D^\pm \to \pi^\pm K^0_S$ decays in Ref. [**?**], evaluated to $O(\epsilon)$ for an infinite and uniform time-acceptance. The asymmetry due to *CP* violation in the neutral kaon sector, governed by Δh, is of approximately the same order of magnitude as the asymmetry due to γ being non-zero. This is illustrated in Fig. **??**, where the expression in Eq. (4.16) is plotted in the default case where $\Delta h = 0$, using the model in Ref. [**?**] to calculate K_i and c_i, as well as including neutral kaon *CP* violation and material interaction effects, calculated using $r_\chi = \epsilon$, with ϵ taking the value in Eq. (4.3). The asymmetry changes significantly when including the latter effects. Therefore, measurements based only on the global asymmetry will suffer relative biases of tens of degrees, not a few degrees, if neutral kaon *CP* violation and material interaction is not taken into account. The contribution to A_{total} due to *CP* violation in the B decay is an order of magnitude smaller than the $O(r_B)$ expectation described in Ref. [**?**] because $\sum_i c_i\sqrt{K_iK_{-i}} \simeq 0.1 \ll 1$. The reason is that $K^0_S\pi^+\pi^-$ is not a *CP* eigenstate and the strong-phase $\Delta\delta_D(s_{-+})$ has a non-trivial phase-space dependence. This results in the CF and DCS interference term, which governs the *CP* asymmetry, changing sign over phase-space and therefore giving a small contribution to the phase-space-integrated yields.

4.2 Detector descriptions for LHCb and Belle II

In order to estimate the effects of *CP* violation and material interaction on γ measurements that are based on the phase-space distribution of signal decays, the equations of Section **??** need to be evaluated to at least $O(r\epsilon)$. Therefore a set of numerical studies are carried out, in which calculations are made to all orders in ϵ, r_χ, r_A and r_B. Furthermore, the bias effects depend on the specific detector material budget and time acceptance of a given experiment. The bias is calculated considering the conditions at the two main flavour physics experiments where measurements of γ will be performed in the next decade: LHCb and Belle II.

4.2.1 LHCb material budget in simulation

- I will need to make a deep dive on LHCb, at the same time motivating a comparison to simpler estimates, in order to show that they are probably ok to use for Belle II

4.2.2 Simplified description of Belle II

Experiment specific biases are obtained for LHCb and Belle II, by assuming time acceptances, momentum distributions, and detector geometries typical of the experiments. The LHCb experiment is a forward arm spectrometer where the B mesons are produced in proton-proton collisions at 13 TeV. Subsequent decays of the K^0_S are highly boosted and can occur within different detector subsystems, which leads to two distinct categories of candidates, with different mean lifetimes and material traversed. Therefore two scenarios are considered for LHCb: one in which the decay products of the K^0_S leave reconstructed tracks in both the silicon vertex detector and downstream tracking detectors (denoted *long-long* or LL), and one in which the decay products of the K^0_S only leave tracks in the downstream tracking detectors (denoted *down-down* or DD). At Belle II, B mesons are produced from decays of $\Upsilon(4S)$ mesons, produced in asymmetric electron-positron collisions. This leads to substantially different decay kinematics in comparison to those found at LHCb. A single scenario is considered for Belle II, because nearly all the K^0_S mesons produced in signal decays in Belle II decay within the tracking volume, with more than 90 % decaying in the vertex detector according to the studies described below. Thus, three scenarios are considered in total: LL LHCb, DD LHCb, and Belle II.

In order to model the experimental time acceptance, the time-dependent integral in Eq. (4.4) is only carried out over a finite time interval (τ_1, τ_2). The intervals are defined for each of the three experimental categories, by requiring that a neutral

kaon, if produced at $x = y = z = 0$ with momentum $p = (p_T, p_z)$, decays within the relevant part of the corresponding detector. The time acceptance has a significant impact for the LHCb categories, where some 20 % of the kaons escape the tracking stations completely before decaying, whereas the resulting cut-off, τ_2, is large enough in Belle II to have negligible significance. A discussion on the exact requirements placed, and corresponding decay lengths, is found in appendix **??**.

The neutral kaon momentum distribution in LHCb is obtained using `RapidSim` [**?**], which can generate decays of B mesons with the kinematic distribution found in LHCb collisions, and falling in the LHCb acceptance. The momentum distribution in Belle II is estimated by decaying B mesons with a momentum of 1.50 GeV/c along the z-axis using `RapidSim`, corresponding to the $\gamma\beta = 0.28$ boost of the centre-of-mass system in Belle II when operated at the $\Upsilon(4S)$ resonance [**?**]. A perfect 4π angular acceptance is assumed. The generated $D \to K^0_S\pi^+\pi^-$ decays are uniformly distributed in phase space. The `RapidSim` samples for LHCb are reweighted to take the relevant time acceptance into account. This is not necessary for Belle II, as all produced K^0_S mesons decay in the tracking volume. The resulting momentum distributions for the three types of sample are shown in Fig. **??**.

The parameter $\Delta\chi$ describes the matter-interaction effect, as detailed in Section **??**. It depends on kaon momentum and varies along a given kaon path, as the kaon intersects detector components made of different materials. In these studies, the calculations are simplified by using a constant set of average material parameters for each experimental scenario. The average material parameters can be estimated for a given experimental scenario by considering the type and length of material traversed by a kaon in the relevant sub-detector(s). A detailed description of the calculation is given in appendix **??**. The average value of the dimensionless parameter $r_\chi = \frac{1}{2}\frac{\Delta\chi}{\Delta\lambda}$, which governs the size of the matter regeneration effect, can be calculated for the three considered experimental scenarios, and the averages are found to satisfy $|r_\chi^{\mathrm{LL}}| = 2.7 \times 10^{-3}$, $|r_\chi^{\mathrm{DD}}| = 2.2 \times 10^{-3}$, and $|r_\chi^{\text{Belle II}}| = 1.0 \times 10^{-3}$.

The LHCb detector is undergoing a significant upgrade prior to the start of the LHC Run 3. However, the material budget and geometry of the relevant sub-detectors will be similar to the sub-detectors used during Run 1 and 2 [**?**, **?**]. Hence the results of this study will be valid for measurements during the upgrade phases of LHCb, even though the detector parameters presented in this section relate to the original LHCb detector.

4.3 Impact on GGSZ measurements of γ: the full study

In the numerical bias studies studies, the amplitude model for $D^0 \to K^0_S\pi^+\pi^-$ decays in Ref. [**?**] is taken to represent the $A_1(s_{+-})$ amplitude. Then $A_2(s_{+-})$ is obtained as described in Section **??**. In terms of A_1 and A_2, the amplitudes $A^{(\overline{D})}_{S(L)}(s_{+-})$ can be expressed and related via Eqs. (4.8) and (4.9), and the full $\mathcal{A}^{\pm}_{S/L}(s_{+-})$ amplitudes calculated for a given set of input parameters $(\gamma^0, r^0_B, \delta^0_B)$. Then Eq. (4.5) gives the kaon state as a function of time, phase-space coordinates, and the material parameter $\Delta\chi$. The neutral kaon state components, $\psi_S(t)$ and $\psi_S(t)$, are inserted into Eq. (4.4), which is integrated numerically over time and the phase-space bins of Fig. **??** to obtain the expected yields in each bin. These integrals use the experimental time acceptance that was described in Section **??**. The signal yields depend on the momentum via the time-acceptance parameters τ_1 and τ_2, and because the material interaction parameter $\Delta\chi$ is momentum dependent. Therefore, the yields are averaged over the K^0_S momentum distributions of LHCb and Belle II. The neutral kaon momentum in the lab frame is correlated with $m^2(\pi^+\pi^-)$, and in order to take this correlation into account in the averaging, the kaon p, p_z, and p_T distributions are extracted for a number of different $m^2(\pi^+\pi^-)$ values, using the `RapidSim` samples described in Section **??**. In order to keep the calculations manageable, the distributions of kaon p, p_z, and p_T for each phase-space point are divided into 5 quantiles and the 5 medians of these quantiles are used to represent the overall distribution.

The parameters $x_\pm$ and $y_\pm$ are determined by a maximum likelihood fit to the calculated yields, using the default yield expression in Eq. (**??**), which ignores the presence of *CP* violation and material interaction in the neutral kaon sector. The fit result and covariance matrix are interpreted in terms of the physics parameters (γ, r_B, δ_B) using another maximum likelihood fit [**?**], to allow for the extraction of the bias $\Delta\gamma = \gamma - \gamma^0$. In the fits, the K_i are obtained using the definition $K_i = K_i^{\text{meas}} = (N^D_i + N^{\overline{D}}_{-i})/(\sum_j N^D_j + N^{\overline{D}}_{-j})$, in terms of the expected yields N^D_i ($N^{\overline{D}}_i$) of a flavour-tagged D^0 ($\overline{D}^0$) decays in bin i of the D decay phase space, calculated as described above for $r^0_B = 0$. This corresponds to experimentally measuring the K_i in a control channel, and takes the effect of neutral kaon *CP* violation and material interaction on K_i measurements into account, as well the experimental time acceptance. The (c_i, s_i) are calculated using $A_1(s_{+-})$ and the experimental time acceptance is taken into account in this calculation as well. While a model-independent method is specifically used here to determine biases, it is expected

that traditional and new unbinned methods such as those in Refs [?, ?, ?, ?, ?, ?, ?, 9] and Ref. [?], respectively, will be similarly biased if the kaon *CP*-violation and regeneration are not accounted for.

4.3.1 Results

The obtained bias $\Delta\gamma$ is shown as a function of input γ^0 for the various experimental conditions in Fig. **??**. The calculations are made using $(r_B^0, \delta_B^0) = (0.1, 130^\circ)$, approximately equal to the physics parameters relevant for $B^\pm \to DK^\pm$ decays [?, ?]. The bias does not vary significantly with γ^0 in the plotted range, which includes the world average value of direct γ measurements as well as the values obtained in full unitarity-triangle fits [?, ?, ?], and for all cases, the bias is found to be below 0.5°, corresponding to relative biases of about half a percent. Thus the biases are of $O(r\epsilon/r_B)$ as expected, given the arguments of Section **??**. The contributions from the individual K^0_S CPV and material interaction effects are also shown. It is seen that the neutral kaon *CP* violation and material interaction effects leads to approximately equal biases in all three cases.

Given the decay-time acceptance and momentum distribution for each experimental category, the mean life time, $\langle\tau\rangle$, of the reconstructed kaons can be calculated. In terms of the K^0_S lifetime $\tau_{K^0_S} = (0.895 \pm 0.004) \times 10^{-11}\,\text{s}$ [?], $\langle\tau_{\text{LL}}\rangle \simeq 0.1\tau_{K^0_S}$ for the LHCb LL category, $\langle\tau_{\text{DD}}\rangle \simeq 0.8\tau_{K^0_S}$ for the LHCb DD category, and at Belle II $\langle\tau_{\text{Belle II}}\rangle \simeq \tau_{K^0_S}$. The difference in average kaon lifetime is reflected in the observed biases, which are found to be larger in the samples with longer lived kaons. The very small effect in the LL category is to be expected because the *CP*-violation effect due to K^0_S not being *CP*-even is approximately cancelled by the *CP*-violation effect arising from $K^0_S - K^0_L$ interference for kaons with decay times much smaller than $\tau_{K^0_S}$ [?]. The time dependence of the bias effect means that it can potentially be beneficial to restrict a measurement to using short-lived K^0_S mesons in a future scenario, where the impact of K^0_S *CP* violation is comparable to the statistical precision of the measurement. For example, the bias can reduced by 40 % in the Belle II scenario if only K^0_S mesons decaying within 8 cm of the beam axis are included in the measurement. This requirement only removes 20 % of the signal yield, and hence only increases the statistical uncertainty of the measurement by 10 %.

The uncertainty bands in Fig. **??** are calculated by repeating the study while varying some of the inputs. The model dependence of the predicted biases is probed by repeating the study using two other amplitude models as input for $A_1(s_{+-})$ and $A_2(s_{+-})$: the model published in Ref. [?] and the model included in EvtGen [?]. The use of different models change the predicted biases by up to 0.05°. When

defining $A_2(s_{+-})$ in terms of $A_1(s_{+-})$, there is an uncertainty due to the unknown (r_k, δ_k) parameters used to describe the $\pi\pi$ resonance terms. This uncertainty is assessed by making the study with 50 different random realisations of the parameter set. The phases δ_k are sampled uniformly in the interval $[0, 2\pi]$ while the r_k are sampled from a normal distribution with $\mu = \tan^2\theta_C$ and $\sigma = \mu/2$. The uncertainty is about 0.05° across the three experiments considered. The studies are repeated while varying the time acceptances and material densities with $\pm 10\,\%$. The largest deviations in biases are found to be below 0.05°. The dependence on the handling of the momentum distribution is estimated by repeating the study using 10 and 20 quantiles to describe the momentum distributions at each point in phase space, instead of 5. The variation in the results is taken as the systematic uncertainty, and found to be below 0.01° for all experiments. There is an additional uncertainty due to the use of simulation samples generated with `RapidSim` to describe the kaon momentum distribution, in lieu of full detector simulations. The uncertainty has not been considered here. Full detector simulation should be used if specific experimental measurements are to be corrected for the biases described in this study.

There is also an uncertainty from the use of (c_i, s_i) as calculated using $A_1(s_{+-})$. It is to be expected that the measured values $(\hat{c}_i, \hat{s}_i)$ from the CLEO collaboration differ by those calculated using $A_1^D(s_-, s_+)$ by terms of $O(\epsilon)$ due to neutral kaon *CP* violation, which is not taken into account in the measurement [**?**]. These corrections can be calculated via a procedure analogous to the one used to estimate the corrections on measurements of γ in this paper. However, as these corrections are much smaller than the experimental uncertainties in the measurement, they have not been studied further.

It is interesting to evaluate the bias obtained if the K_i are calculated from $A_1(s_{+-})$, without any corrections due to neutral kaon *CP* violation and material interaction. If this is done, while the full experimental time acceptance is taken into account, the biases only change by up to 0.01°, across the experiments. This is because the $O(\epsilon)$ corrections in Eq. (4.13), where the expected measured K_i is given to lowest order in ϵ and r_χ, only affect the overall normalisation. If the time acceptance *is not* taken into account, biases of several degrees can occur, irrespective of the presence of neutral kaon *CP* violation or material interaction effects.

While the $B^\pm \to DK^\pm$ decay mode provides the best sensitivity to γ, it is also possible to measure γ in other B decay channels, such as $B^\pm \to D^*K^\pm$, $B^\pm \to DK^{*\pm}$, $B^0 \to DK^{*0}$, and $B^\pm \to D\pi^\pm$. For the purpose of the study presented here, the main difference between the decay channels is that they have different values of r_B and δ_B. Figure **??** shows $\Delta\gamma$ as a function of input δ_B^0, for

$\gamma^0 = 75^\circ$ and three different values of r_B^0. Aside from $r_B^0 = 0.1$, the results are shown for $r_B^0 = 0.005$, which corresponds to the expectation in $B^\pm \to D\pi^\pm$ decays [**?**] and $r_B^0 = 0.25$, which corresponds to $B^0 \to DK^{*0}$ decays [**?**, **?**]. Three features are notable, namely that the biases depend on δ_B^0, that the biases are large for the small $r_B^0 = 0.005$ case, and that the oscillation period of the δ_B dependence is different between the $r_B^0 = 0.005$ case and the $r_B^0 \in \{0.1, 0.25\}$ cases. It is to be expected that $\Delta\gamma$ oscillates as a function of δ_B^0, because δ_B^0 enters the yield equations via $\cos(\delta_B^0 \pm \gamma)$ and $\sin(\delta_B^0 \pm \gamma)$ terms. The r_B^0 dependent behaviour is governed by the relative importance of different $O(r\epsilon)$ correction terms to the phase-space distribution. There are terms of both $O(r_A\epsilon)$ and $O(r_B\epsilon)^2$, which lead to expected biases of size $O(r_A\epsilon/r_B)$ and $O(r_B\epsilon/r_B) = O(\epsilon)$, respectively, cf. the discussion of Section **??**. The $O(r_A\epsilon)$ terms are independent of δ_B^0, whereas the $O(r_B\epsilon)$ terms have factors of $\cos(\delta_B^0 \pm \gamma)$ and $\sin(\delta_B^0 \pm \gamma)$. Therefore the $O(r_A\epsilon)$ and $O(r_B\epsilon)$ terms introduce biases with different dependence on δ_B^0. In the $B^\pm \to D\pi^\pm$ case, the $O(r_A\epsilon)$ correction terms dominate because $r_A/r_B \simeq (0.05/0.005) = 10$. This explains the relatively large bias, as $|r_A\epsilon/r_B^{D\pi}| \simeq 4\%$, and the simple dependence on δ_B^0. The bias is seen to be up to $\pm 1.5^\circ$, but only about $+0.2^\circ$ with the expected value of $\delta_B^{D\pi} \simeq 300^\circ$ [**?**, **?**]. In the $r_B^0 = 0.1$ and $r_B^0 = 0.25$ cases the $O(r_B\epsilon)$ correction terms dominate, and the biases are of $O(\epsilon)$, independent of the r_B^0 value. Therefore both cases have biases of similar size and with similar δ_B^0 dependence. While the input value of $\gamma^0 = 75^\circ$ was chosen for these studies, there is minimal variation in the results if another value of γ^0 in the range $[65^\circ, 85^\circ]$ is used.

The γ measurements treated in this paper can be made using other D-decay final states, such as $D \to K^0_S K^+ K^-$ and $D \to K^0_S \pi^+ \pi^- \pi^0$. The biases from neutral kaon *CP* violation and material interaction on measurements of γ based the D decay phase-space distributions should be of similar size in these decay channels, as those presented for $D \to K^0_S \pi^+ \pi^-$ in this paper. The impact on γ measurements based on the phase-space-integrated yield asymmetry can be expected to be tens of degrees for the $D \to K^0_S K^+ K^-$ channel, where the yield asymmetry is expected to be around 2 %, for the reasons explained in Section **??**. The $D \to K^0_S \pi^+ \pi^- \pi^0$ decay, however, is dominantly *CP*-odd [**?**], and the bias in measurements based on the total asymmetry is therefore expected to be $O(r_B\epsilon)$, ie. a few degrees [**?**]. More precise calculations of the biases would require a repeat of the study included here, with relevant amplitude models and binning schemes in place.

[2]There are similar terms of $O(r_A r_\chi)$ and $O(r_B r_\chi)$, but as ϵ and r_χ are of the same order of magnitude, these terms can be treated completely analogously to the $O(r_A\epsilon)$ and $O(r_B\epsilon)$ terms, and have been left out of the discussion for brevity.

The studies presented here can be used to assign systematic uncertainties to measurements while the statistical uncertainties continue to dominate. As the statistical uncertainty becomes comparable with the bias effects described in this paper, the systematic uncertainty should be assigned by repeating the studies with a detailed detector simulation. This would incorporate a more accurate description of the K^0_S decay-time acceptance, of the full selection criteria, and the traversed material. The detailed calculations can also be used to apply a bias correction if desired.

5

A GGSZ measurement with $B^{\pm} \to Dh^{\pm}$ decays

First I will return to describing the overall strategy a bit, then one can proceed with the data analysis section

5.1 Candidate selection

5.2 Signal and background components

5.3 Measurement of the CP-violation observables

5.4 Systematic uncertainties

5.5 Obtained constraints on γ

6
Conclusions

Say something clever

Bibliography

[1] LHCb collaboration, R. Aaij *et al.*, *Measurement of the CKM angle γ using $B^\pm \to [K^0_S h^+ h^-]_D h^\pm$ decays*, Submitted to JHEP (2020).

[2] M. Bjørn and S. Malde, *CP violation and material interaction of neutral kaons in measurements of the CKM angle γ using $B^\pm \to DK^\pm$ decays where $D \to K^0_S \pi^+ \pi^-$*, JHEP **19** (2020) 106, arXiv:1904.01129.

[3] LHCb collaboration, R. Aaij *et al.*, *Measurement of the CKM angle γ using $B^\pm \to DK^\pm$ with $D \to K^0_S \pi^+ \pi^-$, $K^0_S K^+ K^-$ decays*, JHEP **08** (2018) 176, Erratum ibid. **10** (2018) 107, arXiv:1806.01202.

[4] Y. H. Ahn, H.-Y. Cheng, and S. Oh, *Wolfenstein parametrization at higher order: Seeming discrepancies and their resolution*, Physics Letters B **703** (2011) 571.

[5] L. Wolfenstein, *Parametrization of the Kobayashi-Maskawa Matrix*, Phys. Rev. Lett. **51** (1983) 1945.

[6] Y. Grossman and M. Savastio, *Effects of K-\bar K mixing on determining gamma from B^\pm -> DK^\pm*, Journal of High Energy Physics **2014** (2014) , arXiv: 1311.3575.

[7] M. Gronau and D. Wyler, *On determining a weak phase from charged B decay asymmetries*, Physics Letters B **265** (1991) 172.

[8] M. Gronau and D. London, *How to determine all the angles of the unitarity triangle from Bd0 → DKs andBs0 → Dϕ*, Physics Letters B **253** (1991) 483.

[9] LHCb collaboration, R. Aaij *et al.*, *Measurement of CP violation and constraints on the CKM angle γ in $B^\pm \to DK^\pm$ with $D \to K^0_S \pi^+ \pi^-$ decays*, Nucl. Phys. **B888** (2014) 169, arXiv:1407.6211.

[10] LHCb collaboration, R. Aaij *et al.*, *Measurement of the CKM angle γ using $B^0 \to DK^{*0}$ with $D \to K^0_S \pi^+ \pi^-$ decays*, JHEP **08** (2016) 137, arXiv:1605.01082.